Spectral relaxations of persistent rank invariants

Matt Piekenbrock & Jose Perea

Abstract

Using a duality result between persistence diagrams and persistence measures, we introduce a framework for constructing families of continuous relaxations of the persistent rank invariant for persistence modules indexed over the real line. Like the rank invariant, these families obey inclusion-exclusion, are derived from simplicial boundary operators, and encode all the information needed to construct a persistence diagram. Unlike the rank invariant, these spectrally-derived families enjoy a number of stability and continuity properties typically reserved for persistence diagrams, such as smoothness and differentiability over the positive semi-definite cone. By leveraging its relationship with combinatorial Laplacian operators, we find the non-harmonic spectra of our proposed relaxation encode valuable geometric information about the underlying space, prompting several avenues for geometric data analysis. We investigate the utility of our relaxation with exemplary applications in topological data analysis and machine learning, such as hyper-parameter optimization and shape classification.

1 Introduction

Persistent homology [18] (PH) is the most widely deployed tool for data analysis and learning applications within the topological data analysis (TDA) community. Persistence-related pipelines typically follow a common pattern: given input data set X, construct a filtration (K, f) from X such that useful topological or geometric information may be profitably gleaned from its *persistence diagram*—a multiset summary of f constructed by pairing homological critical values $\{a_i\}_{i=1}^n$ with non-zero *multiplicities* $\mu_p^{i,j}$ [13]:

$$\mathrm{dgm}_p(f) \triangleq \{\, (a_i, a_j) : \mu_p^{i,j} \neq 0 \,\} \cup \Delta, \qquad \mu_p^{i,j} \triangleq \left(\beta_p^{i,j-1} - \beta_p^{i,j}\right) - \left(\beta_p^{i-1,j-1} - \beta_p^{i-1,j}\right) \tag{1.1}$$

By pairing simplices using homomorphisms between homology groups, diagrams demarcate homological features succinctly. The surprising and essential quality of persistence is that this pairing exists, is unique, and is stable under additive perturbations [13]. Whether for shape recognition [9], metric learning [23], dimensionality reduction [33], or time series analysis [29], persistence is the de facto connection between homology and the application frontier.

Though theoretically sound, diagrams suffer from many practical issues: they are sensitive to strong outliers, far from injective, expensive to compute *and* to compare. Tackling some of these issues, practitioners have equipped diagrams with additional structure by way of maps to function spaces—examples include persistence images [1], persistence landscapes [7], and template functions [30]. On the issue of injectivity, Turner et al. propose the *persistent homology transform* (PHT), which is a shape statistic that associates an embedded data set $X \subset \mathbb{R}^d$ with a collection of diagrams sufficient to reconstruct X, sparking both an inverse theory for persistence and a mathematical foundation for metric learning. Though these diagram vectorizations have proven useful for learning applications due to their stability and metric configurability [32], their scalability issue remains limited—not only are diagrams difficult to compute individually, but extending the persistence computation to parameterized settings has proven non-trivial [31].

We seek to shift the computational paradigm on persistence while retaining its application potential: rather than following the construct-then-vectorize approach, we devise a spectral method that performs both steps, simultaneously and approximately. Our strategy is motivated both by a technical observation that suggests advantages exist for the rank invariant computation (section 2.1) and by measure-theoretic results on $\mathbb{R}$-indexed persistence modules [8, 10], which generalize (1.1) to arbitrary *corner points* $(\hat{\imath}, \hat{\jmath}) \in \Delta_+$:

$$\mu_p^{\hat{\imath},\hat{\jmath}}(K, f) \triangleq \min_{\delta > 0} \left(\beta_p^{\hat{\imath}+\delta,\hat{\jmath}-\delta} - \beta_p^{\hat{\imath}+\delta,\hat{\jmath}+\delta}\right) - \left(\beta_p^{\hat{\imath}-\delta,\hat{\jmath}-\delta} - \beta_p^{\hat{\imath}-\delta,\hat{\jmath}+\delta}\right) \tag{1.2}$$

A notable feature of our approach is that it not only avoids explicitly constructing diagrams, but it circumvents the reduction algorithm from [17] entirely. Moreover, our proposed relaxation is *matrix-free*, can be iteratively approximated, is continuously differentiable, and is particularly efficient to compute over parameterized families of inputs due to its spectral formulation.

Contributions: Our primary contribution is the introduction of a several families of spectral rank invariants—$\hat{\mu}_p^*$ and β_p^*—all of which are Lipshitz continuous, stable under relative perturbations, and differentiable on the positive semi-definite cone. By a reduction to spectral methods for Laplacian operators, we also show these invariants are computable in $\approx O(m)$ memory and $\approx O(mn)$ time, where m, n are the number of $p+1, p$ simplices in K, respectively (see section 4). Moreover, both invariants admit iterative $(1-\epsilon)$-approximation schemes, and in both cases are recovered exactly when the parameters ϵ and τ made small enough. Unlike existing dynamic persistence algorithms, our approach is simple in that it requires no complicated data structures or maintenance procedures to implement. Interestingly, our results also imply the existence of an efficient output-sensitive algorithm for computing Γ-persistence pairs with at least $(\Gamma > 0)$-persistence (via [11]) that requires the operator $x \mapsto \partial x$ as its only input, which we consider to be of independent interest.

Outline: We first outline the proposed relaxation, leaving the rest of the paper to discuss the theoretical and practical details associated with using and implementing the relaxation. Informally, we study a family of vector-valued mappings over a *parameter space* $\mathcal{A} \subset \mathbb{R}^d$:

$$(X_\alpha, \mathcal{R}, \epsilon, \tau) \mapsto \mathbb{R}^{O(|\mathcal{R}|)} \tag{1.3}$$

where X_α is an $\mathcal{A}$-parameterized input data set, $\mathcal{R} \subset \Delta_+$ a rectilinear polygon or *sieve* over the upper half-plane Δ_+, and $(\epsilon, \tau) \in \mathbb{R}^2_+$ are approximation/smoothness parameters, respectively. The intuition is that $\mathcal{R}$ is used to filter and summarize the topological and geometric behavior exhibited by X_α for all $\alpha \in \mathcal{A}$, thereby *sifting* the space $\mathcal{A} \times \Delta_+$. The steps to produce this mapping are as follows:

1. Let K denote a fixed simplicial complex constructed from the data set X. Select a parameter space $\mathcal{A} \subset \mathbb{R}^d$ which indexes a continuously-varying filter function f_α of K:

$$(K, f_\alpha) = \{\, f_\alpha : K \to \mathbb{R} \mid f_\alpha(\tau) \leq f_\alpha(\sigma) \;\; \forall\, \tau \subseteq \sigma \in K, \alpha \in \mathcal{A} \,\} \tag{1.4}$$

   Exemplary choices of f_α include filtrations geometrically realized from methods that themselves are have parameters, such as density filtrations or time-varying filtrations over dynamic metric spaces [23].

2. Select a *sieve* $\mathcal{R} \subset \Delta_+$ decomposable to a disjoint set of rectangles $R_1 \cup \cdots \cup R_h$. This choice is application-dependent and typically requires a priori knowledge, though in section 5 we give evidence random sampling may be sufficient for vectorization purposes when $\mathcal{R}$ is unknown.

3. Fix a homology dimension $p \geq 0$ and parameters $(\epsilon, \tau) \in \mathbb{R}^2_+$ representing how *closely* and *smoothly* the relaxation should model the quantity:

$$\mu_p^{\mathcal{R}}(f_\alpha) \triangleq \left\{\, \operatorname{card}\left(\operatorname{dgm}_p(f_\alpha)\big|_{\mathcal{R}}\right) \mid \alpha \in \mathcal{A} \,\right\} \tag{1.5}$$

   We will show in section 3.4, letting both $\tau \to 0$ and and $\epsilon \to 0$ yields the multiplicity function μ_p exactly.

4. Choose a Laplacian operator $\mathcal{L} : C^p(K, \mathbb{R}) \to C^p(K, \mathbb{R})$ to associate to $\mathcal{R}$, such as the *up-*, *down-*, or *combinatorial* Laplacian (optionally normalized [22]). The choice of $\mathcal{L}$ determines how the geometric and topological information about (K, f_α) is encoded.

5. For each corner point (i, j) in the boundary of $\mathcal{R}$, restrict and project $\mathcal{L}$ onto a Krylov subspace:

$$\mathcal{K}_n(\mathcal{L}, v) \triangleq \operatorname{span}\{v, \mathcal{L}v, \mathcal{L}^2 v, \ldots, \mathcal{L}^{n-1} v\}, \qquad v \in \operatorname{span}(\mathbf{1})^\perp$$

   The eigenvalues of $T = \operatorname{proj}_{\mathcal{K}} \mathcal{L}\big|_{\mathcal{K}}$ form the basis of the (ϵ, τ)-approximation[a] of (1.3) (see section 3.2).

[a] Depending on the amount of memory available, step (5) may be accelerated along similar $\alpha \in \mathcal{A}$ by storing the largest $k \geq 0$ eigenvectors of T at each corner point $(i, j) \in \partial(\mathcal{R})$ (see section 4.1 for details).

The remaining steps of the relaxation depend on the application in mind. The duality between diagrams and rank functions suggests any application exploiting vectorized persistence information may benefit from our relaxation; examples include characterizing swarm and flocking behavior with Betti curves [], topology-guided image denoising [], detecting bifurcations in dynamical systems [], generating metric invariants for shape classification and metric learning [], and so on. Moreover, the differentiability of our relaxation enables learning applications seeking to optimize persistence information, such as filtration optimization, incorporating topological priors into loss functions, and....

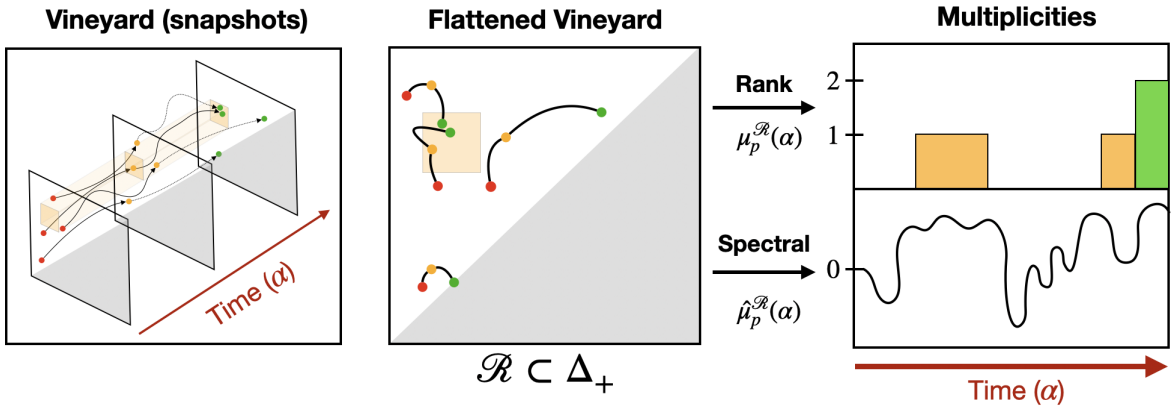

Figure 1: (left) Vineyards analogy depicting diagrams as 'snapshots' over time; (middle) visualization of a rectangular sieve $\mathcal{R} \subset \Delta_+$ (orange) intersecting vines collapsed onto Δ_+; (right) the integer-valued multiplicity function $\mu_p^{\mathcal{R}}(\alpha)$ as a function of time $\alpha \in \mathbb{R}$ (top) and a real-valued spectral relaxation (bottom)

Organization: The paper is organized as follows. Section 2 introduces the notation and background theory on which the rest of the paper depends, including an illuminating derivation of a relatively little-known expression of the persistent Betti number $\beta_p(K)$ in section 2.1, which is a key technical ingredient for much of the work presented here. Section 3.2 contains the main results: a family of spectral relaxations of the rank invariants, their properties and interpretations, and their connections to other areas of mathematics. Section 4 compares and contrasts the computational differences between the proposed relaxation and the traditional persistence computation. Section 5 demonstrates some of the prototypical use cases of the proposed framework. Technical details, illustrative examples, and pseudocode have been relegated to the appendix for readability.

2 Notation & Background

An (abstract) *simplicial complex* $K \subseteq \mathcal{P}(V)$ over a finite *ordered* set $V = \{v_1, v_2, \ldots, v_n\}$ is a collection of simplices $\{\sigma : \sigma \in \mathcal{P}(V)\}$ such that $\tau \subseteq \sigma \in K \implies \tau \in K$. We denote with $K^p = \{\, \sigma \in K : \dim(\sigma) = p \,\}$ the p-simplices of K and by $K^{(p)} = \{\, \sigma \in K : \dim(\sigma) \leq p \,\}$ the p-skeleton of K. A *filtration* $K_\bullet = \{K_i\}_{i \in I}$ of a simplicial complexes indexed by a totally ordered set I is a family of complexes such that $i < j \in I \implies K_i \subseteq K_j$. $K_\bullet$ is called *simplexwise* if $K_j \setminus K_i = \{\sigma_j\}$ whenever j is the immediate successor of i in I:

$$\emptyset = K_0 \subsetneq K_1 \subsetneq \cdots \subsetneq K_m = K_\bullet, \quad K_i = K_{i-1} \cup \{\sigma_i\} \tag{2.1}$$

Equivalently, we may at times define a filtration $K_\bullet$ as a pair (K, f) where $f : K \to I$ is a *filter function* over a totally ordered index set I satisfying $f(\tau) \leq f(\sigma)$ whenever $\tau \subseteq \sigma$, for any $\tau, \sigma \in K$. Here, we consider two index sets: $[n] = \{1, \ldots, n\}$ and $\mathbb{R}$. Note that any filtration may be converted into a simplexwise filtration via *condensing*, *refining*, and *reindexing* maps [2]. For simplicity, but without loss of generality, we exclusively consider simplexwise filtrations and for brevity refer to them as filtrations.

Given a simplicial complex $K \subseteq \mathcal{P}(V)$ and a strictly increasing subset $\sigma = \{v_1, v_2, \ldots, v_{p+1}\} \subseteq V$ satisfying $v_1 < v_2 < \cdots < v_{p+1}$, an *oriented p-simplex* $[\sigma]$ is defined as $[\sigma] = (-1)^{|\pi|} \left[v_{\pi(1)}, v_{\pi(2)}, \ldots, v_{\pi(p+1)}\right]$, where π is a permutation on $[\,p+1\,]$ and $|\pi|$ is the number of inversions of that permutation. The p-boundary ∂_p of an oriented p-simplex $[\sigma] \in K$ is defined as the alternating sum of its oriented co-dimension 1 faces:

$$\partial_p[\sigma] := \sum_{i=1}^{p+1} (-1)^{i-1} [v_1, \ldots, v_{i-1}, v_{i+1}, \ldots v_{p+1}] \tag{2.2}$$

Generalizing beyond simplices, given a field $\mathbb{F}$, an *oriented p-chain* is a formal $\mathbb{F}$-linear combination of oriented p-simplices of K whose boundary $\partial_p[c]$ is defined linearly in terms of its constitutive simplices. We

denote with ∂ the $N \times N$ filtered boundary matrix with respect to an ordered basis $(\sigma_i)_{1 \le i \le N}$ of $K_\bullet$:

$$\partial[i,j] = \begin{cases} (-1)^{s_{ij}} & \sigma_i \in \partial[\sigma_j], \text{ where } s_{ij} = \operatorname{sgn}([\sigma_i], \partial[\sigma_j]) \\ 0 & \text{otherwise} \end{cases} \tag{2.3}$$

Note that ∂_p is completely characterized by the oriented p and $p-1$ simplices of $K_\bullet$ and that one may obtain a matrix representative of ∂_p by setting all columns of ∂ corresponding to simplices of dimension $q \neq p$ to 0. With a small abuse in notation, we will freely use both ∂ and ∂_p to refer to both the boundary operators themselves and their matrix representatives.

For any fixed field $\mathbb{F}$, the collection of p-chains under addition yields an $\mathbb{F}$-vector space $C_p(K)$, whose elements $c \in \partial_p[c']$ are called *boundaries* unless $\partial_p[c] = 0$, in which case they are called *cycles*. Together, the collection of p-boundaries and p-cycles forms the groups $B_p(K) = \operatorname{Im} \partial_{p+1}$ and $Z_p(K) = \operatorname{Ker} \partial_p$, respectively. Since $\partial_p \circ \partial_{p+1} = 0$ for all $p \ge 0$, the quotient space $Z_p(K)/B_p(K)$ is a well-defined group called the *p-th homology group of K* with coefficients in $\mathbb{F}$:

$$H_p(K) \triangleq Z_p(K)/B_p(K), \qquad \beta_p(K) = \dim(H_p(K)) \tag{2.4}$$

The dimension of the p-th homology group $\beta_p(K)$ is called the *p-th Betti number* of K.

Let $K_\bullet = \{K_i\}_{i \in [N]}$ denote a filtration of size $|K_\bullet| = N$, and let $\Delta_+^N = \{(i,j) : 0 \le i \le j \le N\}$ denote the set of filtration index pairs. For every such pair $(i,j) \in \Delta_+^N$, the sequence of inclusions $K_i \subsetneq K_{i+1} \subsetneq \cdots \subsetneq K_j$ induce linear transformations $h_p^{i,j} : H_p(K_i) \to H_p(K_j)$ at the level of homology:

$$0 = H_p(K_0) \to \cdots \to H_p(K_i) \underbrace{\to \cdots \to}_{h_p^{i,j}} H_p(K_j) \to \cdots \to H_p(K_N) = H_p(K_\bullet) \tag{2.5}$$

When $\mathbb{F}$ is a field, this sequence of homology groups uniquely decompose $K_\bullet$ into a pairing (σ_i, σ_j) demarcating the evolution of homology classes [35]: σ_i marks the creation of a homology class, σ_j marks its destruction, and the difference $|i-j|$ records the lifetime of the class, called its *persistence*. The persistent homology groups are the images of these maps and the persistent Betti numbers are their dimensions:

$$H_p^{i,j} = \begin{cases} H_p(K_i) & i = j \\ \operatorname{Im} h_p^{i,j} & i < j \end{cases}, \qquad \beta_p^{i,j} = \begin{cases} \beta_p(K_i) & i = j \\ \dim(H_p^{i,j}) & i < j \end{cases} \tag{2.6}$$

For a fixed $p \ge 0$, the collection of persistent pairs (i,j) together with unpaired simplices (l, ∞) form a summary representation $\operatorname{dgm}_p(K_\bullet)$ called the *p-th persistence diagram of $K_\bullet$*. Conceptually, $\beta_p^{i,j}$ counts the number of persistent pairs lying inside the box $(-\infty, i\,] \times (\,j, \infty)$ (see Figure 2)—the number of persistent homology groups born at or before i that died sometime after j.

2.1 Technical background

The following derivations of the persistent Betti number will be used in proofs and serve as the primary technical motivations for this effort. Given a filtration $K_\bullet$ of size $N = |K_\bullet|$, its p-th persistent Betti number $\beta_p^{i,j}$ at index $(i,j) \in \Delta_+^N$ is defined as follows:

$$\begin{aligned} \beta_p^{i,j} &= \dim\left(Z_p(K_i)/B_p(K_j)\right) \\ &= \dim\left(Z_p(K_i)/(Z_p(K_i) \cap B_p(K_j))\right) \\ &= \dim\left(Z_p(K_i)\right) - \dim\left(Z_p(K_i) \cap B_p(K_j)\right) \end{aligned} \tag{2.7}$$

By definition, the boundary and cycle groups $B_p(K_j)$ and $Z_p(K_i)$ are subspaces of the operators $\partial_p(K_i)$ and $\partial_{p+1}(K_j)$, yielding the following two-term expression:

$$\beta_p^{i,j} = \dim\big(\operatorname{Ker}(\partial_p(K_i))\big) - \dim\big(\operatorname{Ker}(\partial_p(K_i)) \cap \operatorname{Im}(\partial_{p+1}(K_j))\big) \tag{2.8}$$

Now, consider computing $\beta_p^{i,j}$ via (2.8) from matrix representatives $\partial_p \in \mathbb{F}^{n \times m}$. Since the nullity of an operator may be reduced to a rank computation via rank-nullity, the complexity of first term may be reduced

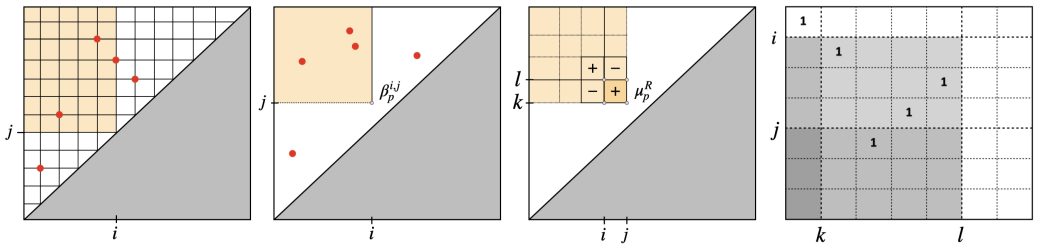

Figure 2: From left to right, $\beta_p^{i,j}$ counts the number of points (3) in upper left-corner of $\mathrm{dgm}_p(K_\bullet)$, where $i,j \in \Delta_+^N$; the same $\beta_p^{i,j}$ with $i,j \in \Delta_+$; the additivity of β_p^* implies μ_p^R over a box $R = [i,j] \times [k,l]$ is given as the sum of four PBNs; generalization of 2.9—in this case $\mu_p^R = 4 - 1 - 0 + 0 = 3$ counts pivot entries in the reduced matrix $R = \partial V$.

to the complexity of computing the rank of a (sparse) $n \times m$ matrix. In contrast, the second [persistence] term typically requires finding a basis in intersection of the two subspaces via either column reductions or projection-based techniques. In general, direct methods that accomplish this require $\Omega(N^3)$ time and $\Omega(N^2)$ memory [20].

There is an alternative approach to computing $\beta_p^{i,j}$ that exploits the structure theorem from [35]. In particular, since 1-parameter persistence modules can be decomposed in an *essentially unique* way into indecomposables, the Pairing Uniqueness Lemma [18] asserts that if $R = \partial V$ decomposes the boundary matrix ∂ to a *reduced* matrix $R \in \mathbb{R}^{m \times n}$ using left-to-right column operations, then:

$$R[i,j] \neq 0 \Leftrightarrow \mathrm{rank}(R^{i,j}) - \mathrm{rank}(R^{i+1,j}) + \mathrm{rank}(R^{i+1,j-1}) - \mathrm{rank}(R^{i,j-1}) \neq 0 \tag{2.9}$$

where $R^{i,j}$ denotes the lower-left submatrix defined by the first j columns and the last $m-i+1$ rows (rows i through m, inclusive). In other words, the existence of non-zero "pivot" entries in R may be inferred entirely from the ranks of certain submatrices of R. One non-obvious consequence of this fact is the following lemma:

Lemma 1. *Given filtration $K_\bullet$ of size $N = |K|$, let $R = \partial V$ denote the decomposition of the filtered boundary matrix $\partial \in \mathbb{F}^{N \times N}$ given in equation (2.3). Then, for any pair (i,j) satisfying $1 \leq i < j \leq N$, we have:*

$$\mathrm{rank}(R^{i,j}) = \mathrm{rank}(\partial^{i,j}) \tag{2.10}$$

Equivalently, all lower-left submatrices of ∂ have the same rank as their corresponding submatrices in R.

An explicit proof of this can be found in [15], though it was also noted in passing by Edelsbrunner [18]. It can be shown by combining (2.9) with the fact that left-to-right column operations preserves the ranks of these "lower-left" submatrices. Though this observation is typically viewed as a minor fact needed to prove the correctness of the reduction algorithm, its implications are quite general, as recently noted by [4]:

Proposition 1 (Bauer et al. [4])**.** *Any persistence algorithm which preserves the ranks of the submatrices $\partial^{i,j}(K_\bullet)$ for all $i,j \in [N]$ is a valid persistence algorithm.*

Indeed, though R is not unique, its non-zero pivots are, and these pivots *define* the persistence diagram. As pointed out in [15], (2.10) in turn enables $\beta_p^{i,j}$ to be written as a sum of ranks of submatrices of ∂_p and ∂_{p+1}:

Proposition 2 (Dey & Wang [15])**.** *Given a fixed $p \geq 0$, a filtration $K_\bullet$ of size $N = |K_\bullet|$, and any pair $(i,j) \in \Delta_+^N$, the persistent Betti number $\beta_p^{i,j}(K_\bullet)$ at (i,j) is given by:*

$$\beta_p^{i,j}(K_\bullet) = |K_i^p| - \mathrm{rank}(\partial_p^{1,i}) - \mathrm{rank}(\partial_{p+1}^{1,j}) + \mathrm{rank}(\partial_{p+1}^{i+1,j}) \tag{2.11}$$

For completeness, we give our own detailed proof of Proposition 2 in the appendix. By combining Proposition 2 with (1.1), we recover a submatrix-rank-based p-th multiplicity function $\mu_p^R(\cdot)$, which to the authors knowledge was first pointed out by Chen & Kerber [11]:

Proposition 3 (Chen & Kerber [11]). *Given a fixed $p \geq 0$, a filtration $K_\bullet = \{K_i\}_{i\in[N]}$ of size $N = |K|$, and a rectangle $R = [i, j] \times [k, l] \subset \Delta_+$, the p-th multiplicity μ_p^R of $K_\bullet$ is given by:*

$$\mu_p^R(K_\bullet) = \operatorname{rank}(\partial_{p+1}^{j+1,k}) - \operatorname{rank}(\partial_{p+1}^{i+1,k}) - \operatorname{rank}(\partial_{p+1}^{j+1,l}) + \operatorname{rank}(\partial_{p+1}^{i+1,l}) \tag{2.12}$$

For more geometric intuition of these propositions, see Figure 2. Note the differences between these two quantities: whereas $\beta_p^{i,j}$ captures points on the diagram that may have unbounded persistence ("essential" classes [18]), the multiplicity function μ_p^R by definition is restricted to classes with bounded persistence[1].

Compared to the classical reduction methods [17, 35], the primary advantage of the rank-based expressions from (2.11)-(2.12) is that they imply the complexity of obtaining either $\beta_p^{i,j}(K_\bullet)$ or $\mu_p^R(K_\bullet)$ may be reduced to the complexity of computing the rank of a set of submatrices of ∂—a fact that actually motivated the rank-based persistence algorithm from Chen et al [11]. Our contributions in this effort stem from the observation that the constitutive terms in these expressions are *unfactored* boundary (sub)matrices—thus, the operation $x \mapsto \partial x$ can be implemented without actually constructing ∂ in memory, enabling the use of e.g. iterative Krylov or subspace acceleration methods [20, 28] for their computation. Indeed, this line of thought suggests other algebraic properties of the rank function—such as invariance under permutations and adjoint multiplication—may simplify these rank-based expressions even further. The rest of the paper explores these questions and their ramifications in detail.

Remark 1. The notation used thus far employed integer indices $(i, j) \in \Delta_+^N$ to describe persistent quantities over a filtration $K_\bullet = (K, f)$ of size $|K| = N$, which is equivalent to indexing K with a filter function $f : K \to I$ defined on the index set $I = [N]$. It is more common in practice to define persistence of a persistent-pair $(\sigma_i, \sigma_j) \in \operatorname{dgm}(K_\bullet)$ via $f(\sigma_j) - f(\tau_i)$, rather than as $j - i$, especially when f is geometric in nature. In this setting, each pair $(\sigma_i, \sigma_j) \in \operatorname{dgm}(K_\bullet)$ is typically represented as the point $(\hat{\imath}, \hat{\jmath})$ where $\hat{\imath} = f(\sigma_i)$ and $\hat{\jmath} = f(\sigma_j)$. Again exploiting the inclusion-exclusion property known for real-valued persistence modules [10], for simplicity we will continue using the notation (i, j) to denote pairs $(i, j) \in \Delta_+$ from the upper-half plane $\Delta_+ = \{(x, y) \in \mathbb{R}^2 : y > x\}$.

3 Spectral relaxation and its implications

3.1 Parameterized boundary operators

In typical dynamic persistence settings (e.g. [14]), the boundary matrix $\partial(K_\bullet)$ must maintain a simplexwise filtration order (w.r.t f_α) to preserve the inclusion structure of $(K_\bullet, f_\alpha)$. In contrast, the rank function is permutation invariant, i.e. for any $X \in \mathbb{R}^{n\times n}$ and permutation P we have:

$$\operatorname{rank}(X) = \operatorname{rank}(P^T X P)$$

This suggests rank computations need not maintain this order—as long as each constitutive term has the same non-zero pattern as its filtration-ordered counterpart, their ranks will be identical. In this section, we show how to adapt the expressions from (2.11) and (2.12) to exploit this permutation invariance.

Let (K, f_α) denote parameterized family of filtrations of a simplicial complex of size $|K^p| = n$. Fix an arbitrary linear extension $(K, \preceq^*)$ of the face poset of K. Define the *$\mathcal{A}$-parameterized boundary operator* $\hat{\partial}_p(\alpha) \in \mathbb{R}^{n\times n}$ of (K, f_α) as the $n \times n$ matrix ordered by $\preceq^*$ for all $\alpha \in \mathcal{A}$ whose entries (k, l) satisfy:

$$\hat{\partial}_p(\alpha)[k, l] = \begin{cases} s_{kl} \cdot f_\alpha(\sigma_k) \cdot f_\alpha(\sigma_l) & \text{if } \sigma_k \in \partial_p(\sigma_l) \\ 0 & \text{otherwise} \end{cases} \tag{3.1}$$

where $s_{kl} = \operatorname{sgn}([\sigma_k], \partial[\sigma_l])$ is the sign of the oriented face $[\sigma_k]$ in $\partial[\sigma_l]$. Observe that (1) the non-zero entries from (3.1) vary continuously in f_α and (2) $\partial_p(\alpha)$ decouples into a product of diagonal matrices $D_*(f_\alpha)$:

$$\hat{\partial}_p(\alpha) = D_p(f_\alpha) \circ \partial_p(K_{\preceq^*}) \circ D_{p+1}(f_\alpha) \tag{3.2}$$

[1] One may always *cone* the filtration to extend μ_p^R to the unbounded case, see [11]

where the non-zero entries of $D_p(f_\alpha)$ and $D_{p+1}(f_\alpha)$ depend on restrictions of f_α to K^p and K^{p+1}, respectively. We refer to the fixed inner matrix $\partial_p \in \{-1, 0, 1\}^{n\times m}$ as the *sign pattern matrix*. Exploiting this decoupling, note that we have an equivalence between the constitutive terms from (2.10) and matrices of the form:

$$\operatorname{rank}\big(\,\partial_p^{i,j}(K, f_\alpha)\,\big) \Leftrightarrow \operatorname{rank}\big(\,\hat{\partial}_p^{i,j}(\alpha)\,\big), \quad \hat{\partial}_p^{i,j}(\alpha) \triangleq D_p(\bar{S}_i \circ f_\alpha) \circ \partial_p(K_{\preceq^*}) \circ D_{p+1}(S_j \circ f_\alpha) \tag{3.3}$$

where $\bar{S}, S : \mathbb{R} \to \{0, 1\}$ are up and down step functions, respectively, of the form $\bar{S}_i(x) = \mathbb{1}_{x>i}(x)$ and $S_j(x) = \mathbb{1}_{x\leq j}(x)$. Since these are discontinuous functions, we may retain the element-wise continuity of (3.2) by exchanging them with clamped *smoothstep* functions $\mathcal{S} : \mathbb{R} \to [0, 1]$ of the form:

$$\mathcal{S}_a^\omega(x) = \begin{cases} 0 & x \leq a \\ P_n\big(\omega^{-1}((a+\omega) - x)\big) & a < x < a + \omega \\ 1 & a + \omega \leq x \end{cases} \tag{3.4}$$

where $P_n : [0, 1] \to [0, 1]$ is a n-th order polynomial satisfying $P_n(0) = 0$ and $P_n(1) = 1$. These functions simply interpolate the discontinuous step portion of S along a fixed interval $(a, a + \omega)$ (see Figure 3).

We summarize these observations with a proposition. Without loss in generality, assume the orientation of the simplices induced by $(K, \preceq^*)$ is inherited from the order on the vertex set V. To simplify the notation, we write $A^x = A^{*,x}$ to denote the submatrix including all rows of A and all columns of A up to x.

Proposition 4. *Let $\delta > 0$ denote the number from (1.2) satisfying $i + \delta < j - \delta$. Given (K, f_α) and any rectangle $R = [i, j] \times [k, l] \subset \Delta_+$ satisfying $i < j \leq k < l$, define the $\mathcal{A}$-parameterized invariants $\beta_p^{i,j} : \mathcal{A} \times K \to \mathbb{N}$ and $\mu_p^R : \mathcal{A} \times K \to \mathbb{N}$ by:*

$$\beta_p^{i,j}(\alpha) = |K_i^p(\alpha)| - \operatorname{rank}\big(\,\hat{\partial}_p^i(\alpha)\,\big) - \operatorname{rank}\big(\,\hat{\partial}_{p+1}^j(\alpha)\,\big) + \operatorname{rank}\big(\,\hat{\partial}_{p+1}^{i+\delta,j}(\alpha)\,\big) \tag{3.5}$$

$$\mu_p^R(\alpha) = \operatorname{rank}\big(\,\hat{\partial}_{p+1}^{j+\delta,k}(\alpha)\,\big) - \operatorname{rank}\big(\,\hat{\partial}_{p+1}^{i+\delta,k}(\alpha)\,\big) - \operatorname{rank}\big(\,\hat{\partial}_{p+1}^{j+\delta,l}(\alpha)\,\big) + \operatorname{rank}\big(\,\hat{\partial}_{p+1}^{i+\delta,l}(\alpha)\,\big) \tag{3.6}$$

yield the correct quantities $\mu_p(R) = \operatorname{card}\Big(\operatorname{dgm}_p(f_\alpha)\big|_R\Big)$ and $\beta_p^{i,j} = \dim(H_p^{i,j}(K))$ from (1.2) and (2.7), respectively, for all $\alpha \in \mathcal{A}$. Moreover, the entries of $\hat{\partial}_p^*(\alpha)$ vary continuously in $\mathcal{A}$.

For completeness, a proof of Proposition 4 is given in the appendix.

Remark 2. In (3.3), we write $\partial_p(K_{\preceq^*})$ (as opposed to $\partial_p(K_\bullet)$ or $\partial_p(K, f)$) to emphasize $\partial_p(K_{\preceq^*})$ is ordered according to the [arbitrary] linear ordering $(K, \preceq^*)$. Note that, in contrast, the boundary terms in proposition 3 are explicitly filtered in the traditional simplexwise manner by f_* (which varies in $\mathcal{A}$). As a result, it is clear that the expressions of persistent rank invariants from (3.5) and (3.6) obtained by replacing the constitutive terms in (2.11) and (2.12) using their parameterized forms from (3.3) are permutation invariant.

3.2 Spectral rank relaxation

Extending from the previous section, we now outline a continuous approximation for the discontinuous rank function. Our approach exploits the ranks spectral characterization: given a matrix $X \in \mathbb{R}^{n\times m}$ and its singular value decomposition (SVD) $X = U\Sigma V^T$, the *rank* of X is given by the composition:

$$\operatorname{rank}(X) = \sum_{i=1}^{n} \operatorname{sgn}_+(\sigma_i(X)), \qquad \operatorname{sgn}_+(x) = \begin{cases} 1 & \text{if } x > 0 \\ 0 & \text{otherwise} \end{cases} \tag{3.7}$$

where $\Sigma = \operatorname{diag}(\{\sigma_1, \sigma_2, \ldots, \sigma_n\})$ are the singular values of X and $\operatorname{sgn}_+ : \mathbb{R} \to \{0, 1\}$ is the one-sided sign function. As the singular values vary continuously under perturbations in X, the discontinuity in (3.7) manifests from the one-sided sign function.

Building off the seminal work of Chen & Mangasarian [25], Bi et al. [6] propose replacing the sgn_+ function in (3.7) with integrated smoothed variations $\hat{\delta}$ of the Dirac delta function δ:

$$(\,\forall\, z \geq 0, \tau > 0\,) \qquad \phi(x, \tau) := \int_{-\infty}^{x} \hat{\delta}(z, \tau)dz, \qquad \hat{\delta}(z, \tau) = \nu(1/\tau) \cdot p\big(z\,\nu(1/\tau)\big) \tag{3.8}$$

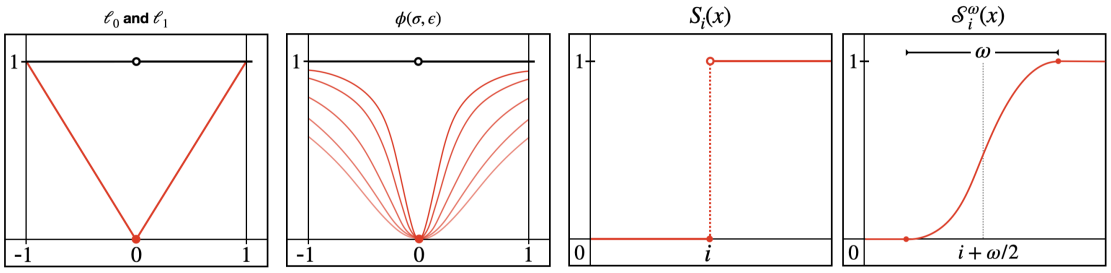

Figure 3: From left to right—the ℓ_1 norm (red) forms a convex envelope over the ℓ_0 (black) pseudo-norm on the interval $[-1, 1]$; $\tilde{\phi}(\cdot, \tau)$ at various values of τ, with $p(x) = 2x(x^2+1)^{-2}$ and $\nu(\tau) = \sqrt{\tau}$ (red) and at $\tau = 0$ (black); the step function $S_i(x)$ from (3.3); the smoothstep relaxation $\mathcal{S}_i^\omega$ from (3.4).

where $p : \mathbb{R}_+ \to \mathbb{R}_+$ is continuous density function and $\nu : \mathbb{R}_+ \to \mathbb{R}_+$ is continuous increasing function satisfying $\nu(0) = 0$ and $\nu(\tau) > 0$. In contrast to the sgn_+ function, if p is continuous on $\mathbb{R}_+$ then $\phi(\cdot, \tau)$ is continuously differentiable on $\mathbb{R}_+$, and if p is bounded above on $\mathbb{R}_+$, then $\phi(\cdot, \tau)$ is globally Lipshitz continuous on $\mathbb{R}_+$. Moreover, note that varying $\tau \in \mathbb{R}_+$ in (3.8) yields an τ-parameterized family of continuous sgn_+ relaxations $\phi : \mathbb{R}_+ \times \mathbb{R}_{++} \to \mathbb{R}_+$, where $\tau > 0$ controls the accuracy of the relaxation.

Many properties of the sign approximation (3.8) extend naturally to the rank function when substituted appropriately via (3.7). In particular, pairing $X = U\Sigma V^T$ with a scalar-valued ϕ that is continuously differentiable at every $\sigma \in \Sigma$ yields a corresponding *Löwner operator* Φ_τ from [5, 6]:

Definition 1 (Spectral Rank Approximation)**.** Given $X \in \mathbb{R}^{n\times m}$ with SVD $X = U\Sigma V^T$, a fixed $\tau > 0$, and any choice of $\phi : \mathbb{R}_+ \times \mathbb{R}_{++}$ satisfying (3.8), define the *spectral rank approximation* $\|\Phi_\tau(X)\|_*$ of X via:

$$\Phi_\tau(X) = \sum_{i=1}^{n} \phi(\sigma_i, \tau) uv^T, \qquad \|\Phi_\tau(X)\|_* = \sum_{i=1}^{n} \phi(\sigma_i, \tau) \tag{3.9}$$

Apart from serving as a smooth approximation of the rank function, this quantity turns out to have a variety of attractive properties related to monotonicity and differentiability, a few of which are recorded below.

Proposition 5 (Bi et al. [6])**.** *The operator $\Phi_\tau : \mathbb{R}^{n\times m} \to \mathbb{R}^{n\times m}$ defined by* (3.9) *satisfies:*

1. *For any $\tau \le \tau'$, $\|\Phi_\tau(X)\|_* \ge \|\Phi_{\tau'}(X)\|_*$ for all $X \in \mathbb{R}^{n\times m}$.*
2. *For any given $X \in \mathbb{R}^{n\times m}$ with rank $r = \text{rank}(X)$ and positive singular values $\Lambda(X) = \{\sigma_1, \sigma_2, \ldots, \sigma_r\}$:*

$$0 \le r - \|\Phi_\tau(X)\|_* \le r \cdot (1 - \phi(\sigma_r, \tau))$$

   Moreover, if τ satisfies $0 < \tau \le \sigma_r/r$, then $r - \|\Phi_\tau(X)\|_*$ is bounded above by a constant $c_\phi(r) \ge 0$.

3. *$\|\Phi_\tau(X)\|_*$ is globally Lipshitz continuous and semismooth[2] on $\mathbb{R}^{n\times m}$.*

Noting property (3), since the sum Lipshitz functions is also Lipshitz, it is easy to verify that replacing the rank function in all of the constitutive terms of both μ_p^R and $\beta_p^{i,j}$ from proposition 4 yields Lipshitz continuous functions whenever the filter function f_α is itself Lipshitz.

Remark 3. It may be shown that Φ_τ is a continuously differentiable operator in $\mathbb{R}^{n\times m}$ for any $\tau > 0$ and is twice continuously differentiable at X if ϕ is twice-differentiable at each $\sigma_i(X)$ for all $i = 1, \ldots, n$ [16]. However, note that $\|\Phi_\tau(X)\|_*$ is not necessarily differentiable on $\mathbb{R}^{n\times m}$ due to Proposition 2.2(e) in [6], but it is differentiable on the positive semi-definite cone $\mathbb{S}_+^n$. This is addressed in the following section.

[2]Here, "semismooth" refers to the existence certain directional derivatives in the limit as $\tau \to 0^+$, see [6, 5].

3.3 Combinatorial Laplacians

For the sake of generality, it is important to make the class of differentiable operators from section 3.2 as large as possible. Noting remark 3, we exploit another well known identity of the rank function:

$$\operatorname{rank}(X) = \operatorname{rank}(XX^T) = \operatorname{rank}(X^T \circ X)$$

As both $\partial_p \circ \partial_p^T$ and $\partial_p^T \circ \partial_p$ are positive semi-definite by definition, studying the spectra of these operators is essentially equivalent to studying the singular values of boundary operators.

The operator given by $\partial_1 \partial_1^T$ is the well known *graph Laplacian* [12]—a natural extension to simplicial complexes has been coined *p-th combinatorial Laplacian* Δ_p, whose explicit representation is given by:

$$\Delta_p(K) = \underbrace{\partial_{p+1} \circ \partial_{p+1}^T}_{L_p^{\text{up}}} + \underbrace{\partial_p^T \circ \partial_p}_{L_p^{\text{dn}}} \tag{3.10}$$

All three operators Δ_p, L_p^{up}, and L_p^{dn} are symmetric, positive semi-definite, and compact—moreover, as shown by [22], their spectra are related by the identities $\Lambda(\Delta_p(K)) \doteq \Lambda(L_p^{\text{up}}) \cup \Lambda(L_p^{\text{dn}})$ and $\Lambda(L_p^{\text{up}}) \doteq \Lambda(L_{p+1})$, where $A \doteq B$ and $A \cup B$ denotes equivalence and union between the *non-zero* elements of the multisets A and B, respectively. Thus, from a rank-based perspective, it suffices to consider any one of these operators.

Without loss of generality, we exclusively consider an $\mathcal{A}$-parameterized variation of L_p^{up}. Following [], we write X^+ to denote the Moore-Penrose pseudoinverse and for brevity write $X^{+/2} = (X^+)^{1/2}$. Using the decoupling observation from (3.2), observe we may write the inner operator from [] as follows:

$$\hat{L}_p^{\text{up}}(\alpha) = D_p^{+/2}(f_\alpha) \circ \partial_p(K_{\preceq^*}) \circ D_{p+1}(f_\alpha) \circ \partial_p(K_{\preceq^*})^T \circ D_p^{+/2}(f_\alpha)$$

Like $\partial_p(\alpha)$, the entries of $\hat{L}_p^{\text{up}}(\alpha)$ vary continuously in α and may be thresholded using smoothstep functions to yield any the constitutive terms from proposition 4. Unlike $\partial_p(\alpha)$, however, the set $\{\, \hat{L}_p^{\text{up}}(\alpha) : \alpha \in \mathcal{A} \,\}$ lies strictly within $\mathbb{S}_+^n$, implying $\|\Phi(\hat{L}_p^{\text{up}})(\alpha)\|_*$ is continuously differentiable. Moreover, Laplacian operators are known to encode rich geometric information in their spectra [22], suggesting several applications may be fruitfully exploit this geometric structure. We give exemplary applications exploiting both facts in section 5.

3.4 Properties & Interpretations

Proposition 6. *Given a simplicial complex K, a filter function $f : K \to \mathbb{R}$, and any τ-parameteried spectral function $\phi : \mathbb{R} \to \mathbb{R}$ satisfying the spectral rank invariants $\hat{\mu}_{p,\tau}^R$ and $\hat{\beta}_{p,\tau}^{i,j}$ satisfy:*

$$\lim_{\tau \to 0^+} \hat{\mu}_{p,\tau}^R = \mu_p^R(K, f), \qquad \lim_{\tau \to 0^+} \hat{\beta}_{p,\epsilon}^{i,j} = \beta_p^{i,j}(K, f)$$

Proof. Use floor / existence argument. □

Proposition 7 (ϕ-monotone)**.** *$\hat{\beta}_p^*$ satisfies, for all $i < j$ and all $k < l$, there exists a non-decreasing function $c_\phi : \mathbb{R} \to \mathbb{R}_+$ whose form depends only on ϕ that obeys the following monotonicity properties:*

$$\begin{aligned} &(\tau = 0) \quad \hat{\beta}_p^{i,k} \le \hat{\beta}_p^{j,k}, \qquad \hat{\beta}_p^{i,k} \ge \hat{\beta}_p^{i,l} \\ &(\tau > 0) \quad \hat{\beta}_p^{i,k} \le \hat{\beta}_p^{j,k} + c_\phi(|i-j|), \qquad \hat{\beta}_p^{i,k} \ge \hat{\beta}_p^{i,l} - c_\phi(|k-l|) \end{aligned}$$

Proof. Use Proposition above part (b) with a specific ϕ. □

Proposition 8. *For any $\tau > 0$ and spectral function $\phi : \mathbb{R} \to \mathbb{R}$ satisfying (3.8), the spectral multiplicity invariant $\hat{\mu}_{p,\tau}^R$ of any rectangle $R = [i, j] \times [k, l] \subset \Delta_+$ obeys the following inclusion exclusion:*

$$\hat{\mu}_{p,\tau}^R(K, f) = \hat{\beta}_{p,\tau}^{j,k} - \hat{\beta}_{p,\tau}^{i,k} - \hat{\beta}_{p,\tau}^{j,l} + \hat{\beta}_{p,\tau}^{i,l}$$

Proof. Use additivity / inclusion exclusion / cancellation property / maybe norm properties of Φ □

Corollary 1. *The* persistence measure *of any simple and connected rectilinear sieve $\mathcal{R} \subset \Delta_+$ with h corner points can be computed using at most $O(h)$ multiplicity evaluations $\hat{\mu}_p^R(K, f)$*

Proof. By the additivity of the multiplicity, we can vertically or horizontally partition any rectangular into two disjoint rectangles and add their total multiplicity to recover the multiplicity of the whole []. Moreover, if $\mathcal{R}$ is simple and hole-free with h corner points, then it is known that it can be decomposed into a minimal set of $h/2 - g - 1 \sim O(h)$ disjoint rectangles (of which several algorithms are known), where g is the number of axis-parallel line segments connecting concave vertices of $\mathcal{R}$ []. □

Regularization: A common approach used in sparse inverse problems to relax the rank function is to impose a regularization scheme. For example, the classical least-squares approach to solving the [possibly ill-posed] linear system $Ax = b$ is often augmented with the *Tikhonov regularization* (TR) for some $\epsilon > 0$:

$$x_\epsilon^* = \underset{x \in \mathbb{R}^n}{\arg\min} \|Ax - b\|^2 + \epsilon \|x\|^2 = (A^T A + \tau I)^{-1} A^T b \tag{3.11}$$

When $\tau = 0$, one recovers the standard ℓ_2 minimization, whereas when $\epsilon > 0$ solutions x^* with small norm are favored. Similarly, by parameterizing ϕ by $\nu(\tau) = \sqrt{\tau}$ and $p(x) = 2x(x^2+1)^{-2}$, one obtains via (3.8):

$$\phi(x, \tau) = \int_0^z \hat{\delta}(z, \tau) dz = \frac{2}{\tau} \int_0^z z \cdot \left((z/\sqrt{\tau})^2 + 1 \right)^{-2} dz = \frac{x^2}{x^2 + \tau} \tag{3.12}$$

Substituting $\text{sgn}_+ \mapsto \phi$ and composing with the singular value function (3.9), the corresponding spectral rank approximation reduces to:

$$\|\Phi_\epsilon(A)\|_* = \sum_{i=1}^n \frac{\sigma_i(A)^2}{\sigma_i(A)^2 + \epsilon} = \text{Tr}\left[(A^T A + \epsilon\, I_n)^{-1} A^T A \right] \tag{3.13}$$

The connection between the TR and the right hand side of (3.13) is now clear: obtaining $\|\Phi_\epsilon(\cdot)\|_*$ is equivalent to n TR-regularized least-squares problems of the form (3.11) where A is substituted with ∂_p (or ∂_p^T) and b is substituted with an α-parameterized p-(co)chain. In this sense, the spectral rank invariants proposed in definition **??** can be viewed as regularized rank invariant approximations.

Remark 4. One interpretation of the relaxation parameter τ is as a bias term that preferences the (pseudo)-inverse towards smaller singular values. Larger values of τ smooth out $\|\Phi_\tau(\cdot)\|_*$ by making the pseudo-inverse less sensitive to perturbations, whereas smaller values of τ lead to a more faithful approximation of the rank. This can be seen directly by (3.11) as well, wherein increasing τ lowers the condition number of $A^T A + \tau I$ monotonically, signaling a tradeoff in stability at the expense of accuracy.

4 Computational Implications

4.1 The Lanczos iteration

Our approach to computing eigen-decompositions is to use a variation of the Lanczos method [24], which estimates eigenvalues by projecting a given linear operator A onto successive Krylov subspaces. That is, given a large, sparse, symmetric $n \times n$ matrix A with eigenvalues $\lambda_1 \geq \lambda_2 > \cdots \geq \lambda_r > 0$ and a vector $v \neq 0$, the order-j Krylov subspaces of the pair (A, v) are the spaces (matrices, respectively) spanned by:

$$\mathcal{K}_j(A, v) \triangleq \text{span}\{v, Av, A^2 v, \ldots, A^{j-1} v\}, \quad K_j(A, v) \triangleq [v \mid Av \mid A^2 v \mid \cdots \mid A^{j-1} v] \tag{4.1}$$

The spectral theorem implies A is orthogonally diagonalizable and that $\Lambda(A)$ may be obtained via successive QR factorizations of $K_j(A, v) = Q_j R_j$ for all $j \in [n]$. Symmetry in A and orthogonality in Q_j imply $q_k^T A q_l = q_l^T A^T q_k = 0$ for all $k > l + 1$, giving the corresponding[3] $T_j = Q_j^T A Q_j$ a tridiagonal structure. As

[3] Unlike the spectral decomposition, there is no canonical choice of T_j due to v being arbitrary, however the iterates $K_j(A, v)$ are related to the full tridiagonalization of A in the sense that if $Q^T A Q = T$ is tridiagonal and $Q = [\, q_1 \mid q_2 \mid \cdots \mid q_n \,]$ is an $n \times n$ orthogonal matrix then $K_n(A, q_1) = Q[\, e_1 \mid Te_1 \mid T^2 e_1 \mid \cdots \mid T^{n-1} e_1 \,]$ is the QR factorization of $K_n(A, q_1)$.

a result, given an initial pair (A, q_1) satisfying $\|q_1\| = 1$, we obtain an orthonormal $Q_j = [\, q_1 \mid q_2 \mid \cdots \mid q_j \,]$ mutually orthogonal to q_{j+1} by restricting and projecting A to its j-th Krylov subspace T_j via:

$$AQ_j = Q_j T_j + \beta_j q_{j+1} e_j^T \;\Leftrightarrow\; \beta_j\, q_{j+1} = Aq_j - \alpha_j\, q_j - \beta_{j\text{-}1}\, q_{j\text{-}1} \qquad (\beta_j > 0) \tag{4.2}$$

where $\alpha_j = q_j^T A q_j$, $\beta_j = \|r_j\|_2$, $r_j = (A - \alpha_j I)q_j - \beta_{j\text{-}1} q_j$, and $q_{j+1} = r_j/\beta_j$. The beauty of the Lanczos method is that if $(q_{j\text{-}1}, \beta_j, q_j)$ are known, then $(\alpha_j,\ \beta_{j+1}, q_{j+1})$ are completely determined, prompting an iterative strategy for building T_j. If A is singular and one encounters $\beta_j = 0$ for some $j < n$, then $\text{range}(Q_j) = \mathcal{K}_j(A, q_1)$ is an A-invariant subspace, the iteration stops, and the symmetric eigenvalue problem is solved as $\Lambda(T_j) = \Lambda(A)$ and $j = \text{rank}(A)$.

The Lanczos iteration and its many variants are part of a family of so-called "matrix free" spectral methods—the only aspect of the computation that depends on A is the matrix-vector product operator $v \mapsto Av$. Indeed, as A is not modified during the computation, the iteration may be executed without explicitly storing A in memory. Moreover, the three-term recurrence from (A.21) implies each iteration requires just three $O(n)$-sized vectors and a few $O(n)$ vector operations, leading to the following result:

Lemma 2 ([28, 34])**.** *Given a symmetric rank-r matrix $A \in \mathbb{R}^{n\times n}$ whose matrix-vector operator $A \mapsto Ax$ requires $O(\eta)$ time and $O(\nu)$ space, the Lanczos iteration computes $\Lambda(A) = \{\lambda_1, \lambda_2, \ldots, \lambda_r\}$ in $O(\max\{\eta, n\} \cdot r)$ time and $O(\max\{\nu, n\})$ space, when computation is done in exact arithmetic.*

As in [28], the assumption of exact arithmetic simplifies both the presentation of the theory and the corresponding complexity statements. Although this assumption is unrealistic in practical settings, it yields a grounded expectation of what is possible to achieve in the *finite-precision* regime: any implementation that computes $\Lambda(A) = \{\lambda_1, \lambda_2, \ldots, \lambda_j\}$ using the Lanczos iteration in finite-precision arithmetic exhibits $\Omega(\max\{\eta, n\} \cdot j)$ time and $\Omega(\max\{\nu, n\})$ space complexity.

In practice, finite-precision arithmetic introduces both rounding and cancellation errors into the computation, which manifests as loss of orthogonality between the Lanczos vectors. These errors not only affect the methods convergence rate towards an invariant subspace, but in fact they muddle the termination condition entirely. As a result, several decades of research have been dedicated to developing orthogonality-enforcement schemes that retain the simplicity of the Lanczos iteration without increasing either the time or space complexities by non-trivial factors. As these extensions are complex, multifaceted, and beyond the scope of the present work, we defer their discussion to the appendix A.3 and refer the curious reader to [20, 28, 34] and references therein for an overview.

4.2 The combinatorial Laplacian `matvec`

The efficiency of the Lanczos method depends crucially on the existence of the three-term recurrence and a fast matrix-vector (`matvec`) operator, the former of which arises in the decomposition of symmetric matrices while the latter depends on the structure of A. For general symmetric matrices $A \in \mathbb{R}^{n\times n}$, Lanczos requires $O(n\nu r)$ operations per iteration when A has an average of ν nonzeros per row [20]. When A is a graph Laplacian $L = \partial_1 \partial_1^T$ this is markedly improved, as the $x \mapsto Lx$ operation is linear in $|E|$ due to the graph structure. It is not immediately clear whether these improvements generalize to combinatorial Laplacian operators derived from simplicial complexes—our first result of of this section generalizes this algorithm.

Lemma 3. *For any $p \geq 0$ and simplicial pair (K, f), if there exists an indexing function $h : K^p \to [n]$ with $O(1)$ access time and $O(c)$ storage, then there exists a two-phase algorithm for computing the inner product $x \mapsto \langle\, L_p, x \,\rangle$ in $O(m(p+1))$ time and $O(\max(c, m))$ storage, where $n = |K^p|$ and $m = |K^{p+1}|$.*

The algorithm and proof are given in appendix section A.1. From a practical perspective, many hash table implementations achieve expected $O(1)$ access time using only a linear amount of storage, and as $p \geq 0$ is typically quite small—typically no greater than two—implying the operation $x \mapsto Lx$ in practice exhibits $\approx O(m)$ time and space complexities. As more concrete statements about the computation require moving beyond asymptotic analysis, we delegate the practical details—along with pseudocode of the two-phase algorithm—to appendix C, for the computationally-minded reader. Combining lemma 3 with proposition 10,

Proposition 9. *For any small constant $p \geq 0$, the spectra $\Lambda(L_p)$ of a rank-r combinatorial Laplacian operator $L_p : \mathbb{R}^n \to \mathbb{R}^n$ derived from a simplicial complex K with $n = |K^p|$ and $m = |K^{p+1}|$ can be computed in $O(mr)$ time and $O(m)$ storage via the Lanczos iteration when carried out in exact arithmetic.*

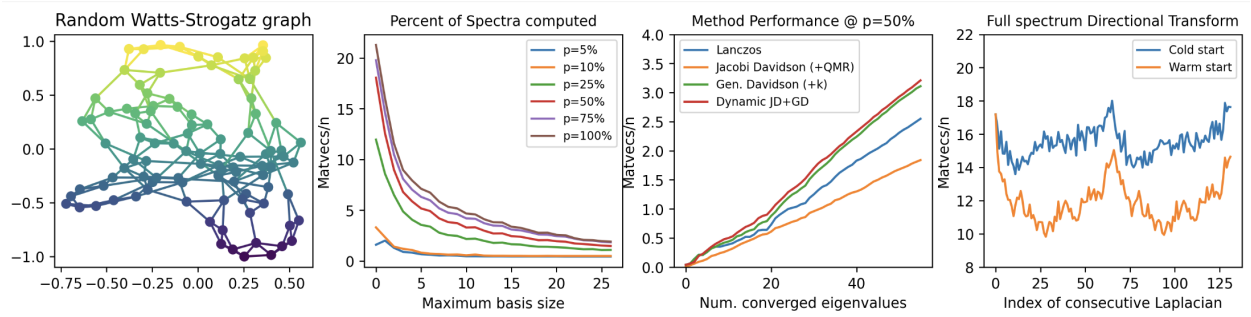

Figure 4: Random Watts-Strogatz "Small world" graph example

Remark 5. The standard reduction-family of algorithms computes the p-th persistent homology of a simplicial complex K of size $N = |K|$ in $O(N^3)$ time and $O(N^2)$ space, respectively. These bounds have been shown to be tight $\Theta(N^3)$ on certain pathological inputs []. Interestingly, Chen and Kerber [11] have shown that since the persistence diagram contains at most $N/2 = O(N)$ points, it may be constructed using at most $2n - 1$ "μ-queries" (μ_p^R) via a divide-and-conquer scheme on the index-persistence plane—thus, via Proposition 9, we may construct the full diagram using this approach with the same $O(N^3)$ complexity.

4.3 Rank computation

The first and most general application of the work presented here is the matrix-free computation of persistent rank invariants in effectively $O(n^2)$ time and $O(m)$ storage, where $n = |K^p|$ and $m = |K^{p+1}|$. To demonstrate this empirically, we sampled 30 random graphs according to the Watts-Strogatz [] rules with parameters $n = 500, k = 10, p = 0.15$. These graphs tend to exhibit 'small world' characteristics inherited by many real-world networks, such as social networks, gene networks, and transportation networks. For our purposes, since the graph distance between pairs of nodes scale logarithmically with the size of the graph, we ensure the sampled random graphs to be uniformly sparse. The corresponding incidence matrix $\partial_1 \in \mathbb{R}^{n\times m}$ and up-Laplacians $L_0^{\text{up}} \in \mathbb{R}^{n\times n}$ would have $\approx 5,000$ and $\approx 5,500$ non-zero entries, were they to be formed explicitly, which are weighted according randomly by embedding the graph in the plane and filtering graph via its sublevel sets in a random direction. A much smaller Watts-Strogatz graph of the same type (but with only 50 nodes) is shown on the left-side of figure 4, colored by the filtering of its lower stars. To test the scability of the laplacian operator studied here, we computed various percentages of the spectra of these 30 graphs via iterative methods discussed in section **??** and reported various of their time- and storage- related statistics in figure 4. All statistics reported are the average statistics collected from all 30 random graphs, which were collected using various iterative methods implemented the PRIMME software []. On the far left of figure 4, we display a random metric embedding of a small Watts-Strogatz graph to convey the structure of the type of graphs we consider.

Storage requirements: On the left side of figure 4 next to the example network model, we record the ratio of `matvec` operations (relative to n) needed to compute p% of the spectrum as a function of the maximum number basis vectors kept in-memory for reorthogonalization purposes. The ideal Lanczos method needs just 3 such vectors in exact arithmetic due to the three-term recurrence, justifying the space complexity record in 10; in contrast, with finite-precision arithmetic, one needs additional basis vector to ensure the orthonormality of the eigenvectors to machine precision. Each additional basis vector simultaneously increases both the cost of performing a Lanczos step and the accuracy of the orthogonalization, which subsequently decreases the number of total `matvec` operations needed. As one can see from the plot, having $\approx 20 - 25$ basis vectors is more than enough to ensure the ratio of `matvec` operations is kept to a small constant (in this case, less than 5) when approximating any portion of the spectra. This justifies our claim that combinatorial Laplacian operators, for many real-world data sets, requires just $O(m)$ memory complexity to compute eigenvalues (and thus, the persistent rank invariants).

Time requirements: The remaining two figures on the right side of figure 4 show the same ratio of `matvecs`/n—effectively the constant associated with quadratic time complexity statement in 10

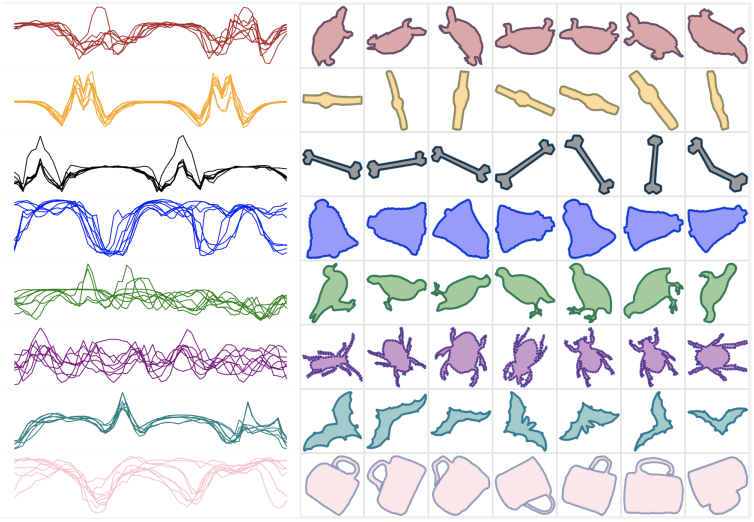

5 Applications & Experiments

5.1 Shape comparison

In general, both combinatorial and topological aspects of a given topological space are encoded in the spectra of Laplacian operators. For example, the Laplacians of a simplicial complex encode its basic topology via its homology groups, which is characterized by the nullspace of the corresponding operator—this is identical for most of the Laplace operators, whether they are normalized, weighted, signless, and so on []. In contrast, these operators differ in the nonzero part of the spectrum, which when equipped with a scalar-product encode specific geometric features in addition to topological properties.

5.2 Filtration optimization

A common setting in topological data analysis is the setting wherein one has access to a means of building a filtration (K, f) where $f : K \to \mathbb{R}$ is a filter function satisfying $f(\tau) \leq f(\sigma)$ for all $\tau \subseteq \sigma \in K$, but the filter function f itself is parameterized by some hyper-parameters. For example, a common setting is the one where the data set (X, d_X) comes equipped with some notion of density $f : X \to \mathbb{R}_+$, and one would like to build a persistence diagram on d_X in a way that is robust to local fluctuations in density. This is a common practical setting often encountered in practice, as it is known that persistence is unstable with respect to *strong outliers* [], which prevents persistent homology from detecting a spaces prominent underlying topological structure, when it exists. Most work seeking to remedy this issue proceeds by either (1) removing such outliers according to some heuristic [], (2) transforming the metric to lessen the importance of such points in the persistence diagram [], or (3) creating a 2-parameter persistence module with one dimension filtered by (co)-density. Of the three, (1) is ultimately a heuristic not useful for complex data sets as it discards important data; (2) imposes a parameter that must be set to proceed, and (3) is perhaps ideal but currently considered both analytically and computationally intractable in practice.

To illustrate an alternative approach to the ways mentioned above, consider a fixed Delaunay complex K built on a set of points sampled noisily around S^1 in the plane, shown in figure 5. Ultimately, we would like to detect the presence of the circle in X via its persistence diagram, as that is the original purpose of persistence []. We reframe the problem as follows: rather than filtering K according to its ambient metric d_X, we ask first whether there *exists* significant topological information at any density scale α. Generically, we consider the following optimization problem:

$$\alpha^* = \arg\max_{\alpha \in \mathbb{R}} \ \mu_p(K, f_\alpha)\big|_R \tag{5.1}$$

If there exists a density scale $\alpha \in \mathbb{R}_+$ wherein a cycle $c \in H_1(K; \mathbb{R})$ is highly persistent and $R \subset \Delta_+$ is appropriately chosen, then any maximizer of (5.1) yields an appropriate density scale α^* with which to

detect the topology of the data. From another perspective, we refer to this process of choosing appropriate filtration (hyper-)parameters to yield persistence information as *filtration optimization*.

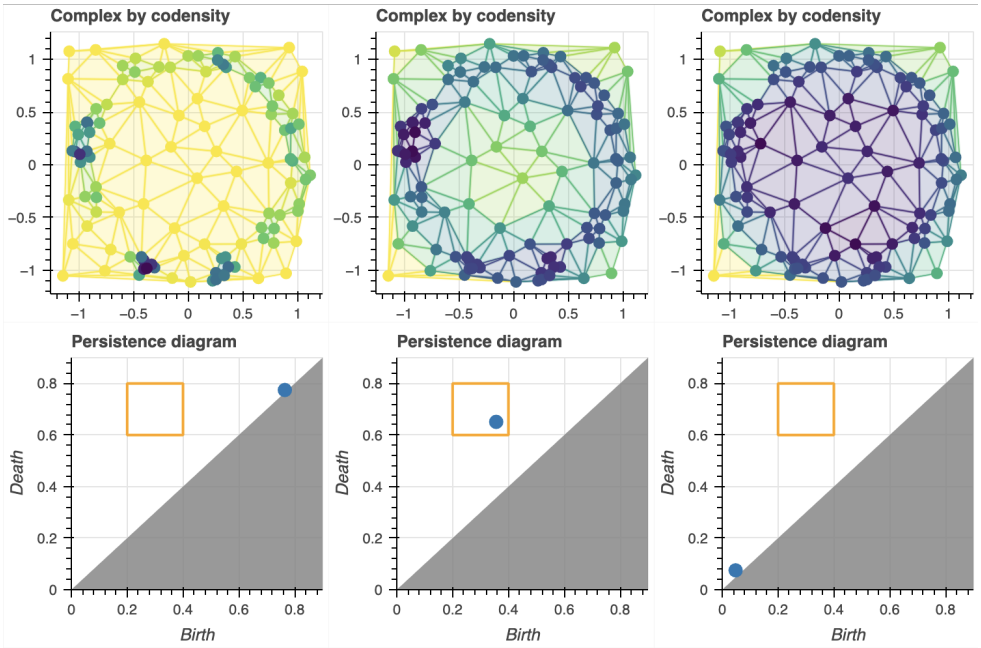

Figure 5: A fixed Delaunay complex filtered by a kernel (co)density estimate for different bandwidth parameters α. Observe that either too small (left) or too large (right) a choice of bandwidth can obscure the underlying topological structure, whereas an appropriate choice of bandwidth creates a filtration that detects the underlying circle.

As an introductory example, we sampled 80 points noisily around S^1 and then sampled an additional 30 points in $[-1,1] \times [-1,1]$ to act as "strong outliers." After constructing a Delaunay complex K of these points, we parameterized a filter function $f_\alpha : K \times \mathbb{R} \to \mathbb{R}_+$ by assigning the filtration values of each simplex according to the lower stars of a kernel (co)density estimate, upon which we computed its vineyard [14] along a subset $\mathcal{A} \subset \mathbb{R}$. The vineyard, colored by α, is shown on the left side of figure 6. In this example, we choose the rectangle $R = \frac{1}{5}([1,2] \times [3,4])$ out of simplicity; the corresponding multiplicity function is shown in the black curve on the right of figure 6. By inspection, the optimal density parameter satisfying (5.1) is any parameter α lying approximately in the interval $[0.40, 0.44]$. Observe that any first-order optimization procedure initialized in the interval $\alpha_0 \in [0.3, 0.5]$ yields a maximizer $\hat{\alpha}$ in the interval $[0.36, 0.46]$, which is quite close to the interval $[0.40, 0.44]$. In this toy example, this is sufficient, however if a better estimate was required (e.g. the multiplicity was required to be positive as a constraint) then observe one could iteratively shrink ϵ to obtain a better approximation of μ_1, and then repeat the first-order optimization. This is synonymous to the *iterative thresholding* techniques often in high-dimensional statistics and machine learning, see [] for an overview.

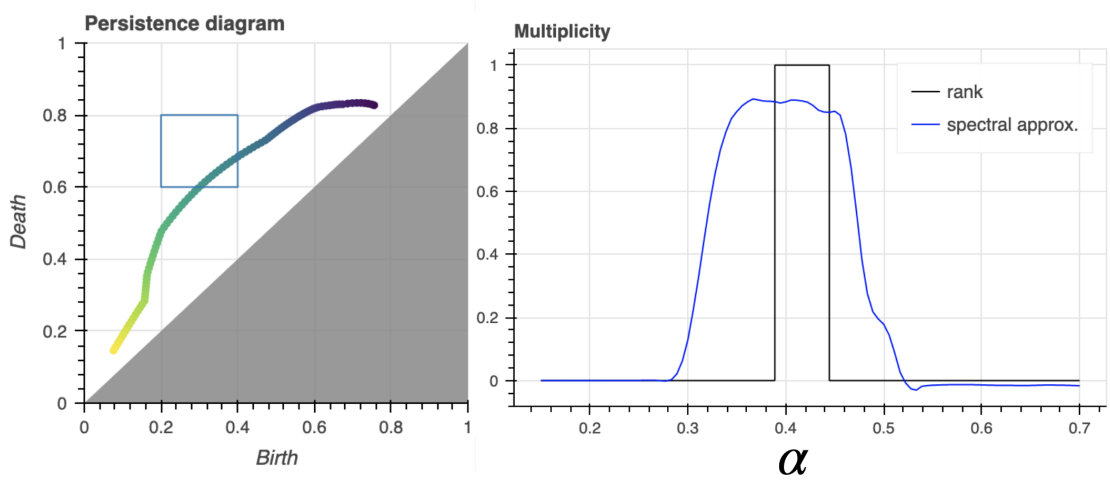

Figure 6: (Left) Vineyard of of the codensity α-parameterized filtration from figure 5. (Right) The exact multiplicity $\mu_1(K, f_\alpha)$ (black) and the proposed spectral relaxation (smoothed, blue) with relaxation parameter $\epsilon = 1\text{e}{-3}$.

A Appendix

Expanded Intro

Though homology is primarily studied as a topological invariant, the fact that persistent homology encodes both topological and geometric information in its diagram has motivated its use not only as a shape descriptor but also as a metric invariant. Metric invariants, or "signatures," are commonly used in metric learning to ascertain whether two comparable data sets X, Y represent the same object—typically up to a some notion of invariance. One mathematically attractive model for measuring the dissimilarity between shapes/datasets is the Gromov-Hausdorff (GH) distance $d_{\text{GH}}((X, d_X), (Y, d_Y)$ between compact metric spaces $(\mathcal{X}, d_X), (\mathcal{Y}, d_Y)$: by altering the choice of metric (d_X, d_Y), the corresponding metric-distance d_{GH} can be adapted to a chosen notion of invariance [] or to increase its discriminating power []. Though it is NP-hard to compute [], the GH distance defines a metric on the set of isomorphism classes of compact metric spaces endowed with continuous real-valued functions, justifying its study as a mathematical model for shape matching and metric learning. Moreover, it is known that the GH distance is tightly lower-bounded by the bottleneck distance between persistence diagrams constructed over Rips filtrations $R(X, d_X), R(Y, d_Y)$ [], which can be computed in polynomial time. Indeed, Solomon et al [] showed distributed persistence invariants characterize the quasi-isometry type of the underlying space, allowing one to provably interpolate between geometric and topological structure.

Though theoretically well-founded and information dense, persistence diagrams come with their own host of practical issues: they are sensitive to strong outliers, far from injective, and their de-facto standard computation exhibits high algorithmic complexity. Moreover, the space of persistence diagrams $\mathcal{D}$ is a Banach space, preventing one from doing even basic statistical operations, such as averaging []. As a result, many researchers have focused on extending, enhancing, or otherwise supplementing persistence diagrams with additional information. Turner et al [] proposed associating a collection a shape descriptors with a PL embedded $X \subset \mathbb{R}^d$—one descriptor for each point on S^{d-1}—which they called a *transform*. More exactly, suppose both the data X and its geometric realization K are PL embedded in $\mathbb{R}^d$ and has centered and scaled appropriately. The main theorem in [] is that associating a persistence diagram, or even a simpler descriptor such as the Euler characteristic, for every point on S^{d-1} is actually sufficient information to theoretically reconstruct K.

Missing from the above work is the are two important directions: how do you configure such transforms to retain the important topological/geometric information and discard irrelevant information, and (2) how may we efficiently compute them? The former question is synonymous with choosing the invariance model in the GH framework, which seems to be highly domain specific. In the latter case, though we know the

number of directions is bounded [], the bound is simply too high to be of any practical use. While there are efficient algorithms for both the ECC and persistence computations in static settings, the state of the art in parameterized settings is non-trivial and ongoing research area.

Expanded Background

Laplacian Energy: Ever since Kirchoff's matrix tree theorem, which relates any cofactor of the graph Laplacian to the number of spanning trees of a graph.... functions summarizing the spectra of Laplacian operators with a scalar value have found many applications, from quantifying hierarchical image complexities, to summarizing electrical resistance between vertices in a circuit network, to indicating the melting or boiling point of certain polycyclic aromatic hydrocarbons in chemical applications []. More generally, the sum of the largest k eigenvalues of L is related to the clique number of the graph, as a measure of complexity. is often termed the *Laplacian energy*, has used

Letters

As topological invariants, Betti numbers are invariant under homeomorphisms: any pair of filtrations (K, f) and (K', f') that are homotopy equivalent have identical homology classes and thus isomorphic persistence diagrams. This invariance can be a useful thing at the level of homology, as non-homeomorphic spaces can sometimes be differentiated by inspecting differences between their corresponding homology classes. However, invariance under homeomorphisms can at times discard geometric information that may be useful for differentiating objects. For example, consider creating a classifier for the alphabet of English characters in the font shown below:

A B C D E F G H I J K L M N O P Q R S T U V W X Y Z

If one were to triangulate images of each of the letters shown above and compute their Betti numbers, one would find just three homology classes: one class for those letters that have two holes (B), one class of letters that have one hole (A, D, O, P, Q, and R), and one class for the rest of the letters, which collapse to points. Thus, if one were concerned with differentiating letters of the alphabet, one may conclude that homology is not simply not strong enough of an invariant to do so.

It would be beneficial to have an invariant that was sensitive to the geometries between shapes, but also stable in some sense.

A.1 Combinatorial Laplacians

Continuing the theme of studying invariances of the rank function to simplify expressions (2.11) and (2.12), in this section we exploit another well known identity of the rank function for zero characteristic fields:

$$\operatorname{rank}(X) = \operatorname{rank}(XX^T) = \operatorname{rank}(X^TX)$$

On the spectral side, it is well-known the square roots of the non-zero eigenvalues of either XX^T or X^TX yield the singular values of X. Since $\partial_1\partial_1^T$ is the well studied *graph Laplacian*, we may consider the study of spectra of *combinatorial Laplacians*—generalizations of the graph Laplacian—as the study of singular values of boundary operators.

The natural extension of the graph Laplacian L to simplicial complexes is the *p-th combinatorial Laplacian* Δ_p, whose explicit matrix representation is given by:

$$\Delta_p(K) = \underbrace{\partial_{p+1} \circ \partial_{p+1}^T}_{L_p^{\text{up}}} + \underbrace{\partial_p^T \circ \partial_p}_{L_p^{\text{dn}}} \tag{A.1}$$

Indeed, when $p = 0$, $\Delta_0(K) = \partial_1\partial_1^T = L$ recovers the graph Laplacian. As with boundary operators, $\Delta_p(K)$ encodes simplicial homology groups in its nullspace, a result known as the discrete Hodge Theorem []:

$$\tilde{H}_p(K;\mathbb{R}) \cong \ker(\Delta_p(K)), \quad \beta_p = \operatorname{nullity}(\Delta_p(K)) \tag{A.2}$$

The fact that the Betti numbers of K may be recovered via the nullity of $\Delta_p(K)$ has been well studied (see e.g. Proposition 2.2 of []). In fact, as pointed out by [], one need not only consider Δ_p as the spectra of Δ_p, L_p^{up}, and L_p^{dn} are intrinsically related by the identities:

$$\Lambda(\Delta_p(K)) \doteq \Lambda(L_p^{\text{up}}) \dot{\cup} \Lambda(L_p^{\text{dn}}), \qquad \Lambda(L_p^{\text{up}}) \doteq \Lambda(L_{p+1}^{\text{dn}}) \tag{A.3}$$

where $A \doteq B$ and $A \dot{\cup} B$ denotes equivalence and union between the *non-zero* elements of the multisets A and B, respectively. Moreover, all three operators Δ_p, L_p^{up}, and L_p^{dn} are symmetric, positive semidefinite, and compact—thus, for the purpose of estimating β_p, it suffices to consider only one family of operators.

To translate the continuity results from definition **??** to any of the Laplacian operators above, we must consider weighted versions. Here, a *weight function* is a non-negative real-valued function defined over the set of all faces of K:

$$w : K \to \mathbb{R}_+ \tag{A.4}$$

The set of weight functions and the choice of scalar product on $C^p(K,\mathbb{R})$ wherein elementary cochains are orthogonal are in one-to-one correspondence [] (see Appendix A.1). In this way, we say that the weight function *induces* an inner product on $C^p(K,\mathbb{R})$:

$$\langle\, f, g \,\rangle_w = \sum_{\sigma \in K^p} w(\sigma) f([\sigma]) g([\sigma]) \tag{A.5}$$

Moreover, Laplacian operators are uniquely determined by the choice of weight function. This correspondence permits us to write the matrix representation of Δ_p explicitly:

$$\Delta_p(K,w) \triangleq W_p^+ \partial_{p+1} W_{p+1} \partial_{p+1}^T + \partial_p^T W_p^+ \partial_p W_{p+1} \tag{A.6}$$

where $W_p = \operatorname{diag}(\{\, w(\sigma_i) \,\}_{i=1}^n)$ represents a non-negative diagonal matrices restricted $\sigma \in K^p$ and W^+ denotes the pseudoinverse. Note that (A.6) recovers (A.1) in the case where w is the constant map $w(\sigma) = 1$, which we call the *unweighted* case.

Unfortunately, various difficulties arise with weighting combinatorial Laplacians with non-constant weight functions, such as asymmetry, scale-dependence, and spectral instability. Indeed, observe that in general neither terms in (A.6) are symmetric unless $W_p = I_n$ (for L_p^{up}) or $W_{p+1} = I_m$ (for L_p^{dn}). However, as noted in [26], L_p^{up} may be written as follows:

$$L_p^{\text{up}} = W_p^+ \partial_{p+1} W_{p+1} \partial_{p+1}^T = W_p^{+/2} \big(W_p^{+/2} \partial_{p+1} W_{p+1} \partial_{p+1}^T W_p^{+/2} \big) W_p^{1/2} \tag{A.7}$$

Since (A.7) is of the form W^+PW where $P \in S_n^+$ and W is a non-negative diagonal matrix, this rectifies the symmetry problem. Towards bounding the spectra of L_p^{up}, Horek and Jost [] propose *normalizing* Δ_p by augmenting w's restriction to K^p:

$$w(\tau) = \sum_{\tau \in \partial(\sigma)} w(\sigma) \quad \forall\, \tau \in K^p,\, \sigma \in K^{p+1} \tag{A.8}$$

Substituting the weights of the p-simplices in this way is equivalent to mapping $W_p \mapsto \mathcal{D}_p$ where $\mathcal{D}_p$ is the *diagonal degree matrix*. The corresponding substitution in (A.7) yields the *weighted combinatorial normalized Laplacian* (up-)operator:

$$\mathcal{L}_p^{\text{up}} = (\mathcal{D}_p)^{+/2} \partial_p W_{p+1} \partial_p^T (\mathcal{D}_p)^{+/2} = \mathcal{I}_n - \mathcal{A}_p^{\text{up}} \tag{A.9}$$

where $\mathcal{A}_p^{\text{up}}$ is a weighted adjacency matrix, and $\mathcal{I}_n$ is the identity matrix with $\mathcal{I}(\tau) = \text{sign}(w(\tau))$ (see Section 4.2). The primary benefit of this normalization is that it guarantees $\Lambda(\mathcal{L}_p^{\text{up}}) \subseteq [0, p+2]$ for any choice of weight function, from which one obtains several useful implications, such as tight bounds on the spectral norm []. The same results holds for up-, down-, and combinatorial Laplacians. Moreover, as we will show in a subsequent section, one obtains stability properties with degree-normalization not shared otherwise.

Remark 6. Compared to (A.7), is it worth remarking that one important quality lost in preferring $\mathcal{L}_p^{\text{up}}$ over L_p^{up} is diagonal dominance.

Inner Products

Though the general Laplacian operator carries with it an interpretation of its eigensets as representing information about the intersection pattern of the underlying complex, a more precise interpretation of the eigensets depends both the operator and weighting scheme in question. Many early results followed Kirchhoff's observations about the properties of L reflecting certain physical laws of electrical flows in circuit networks, wherein eigenvectors have certain interpretations useful for graph sparsification and graph partitioning [12]. More recently, Nadler observed the *normalized* graph Laplacian given by:

$$\mathcal{L} = D^{-1/2}(D - A)D^{-1/2} \tag{A.10}$$

connects the process of diffusion (over a probability density) to the eigensets to $\mathcal{L}$. Yet another choice of normalization relates the eigenfunctions of $\mathcal{L}$ to the discrete Laplace–Beltrami operator on manifolds [], which carries a certain "heat" interpretation with it. Ultimately, just as persistence diagrams encode geometric interpretations through their domain-specific filter functions, the geometry contained in the spectra of combinatorial Laplacians is reflected by the choice of a domain-specific weight function.

Weight functions may be interpreted through their action on the coboundary vector space $C^p(K, \mathbb{R}) := \text{Hom}(K, \mathbb{R})$. As with $C_p(K, \mathbb{R})$, a basis for $C^p(K, \mathbb{R})$ is given by the set of its *elementary cochains*:

$$\{\, \chi([\sigma]) \mid [\sigma] \in B_p(K, \mathbb{R}) \,\}, \text{ where } \chi([\sigma']) = \begin{cases} 1 & \text{if } [\sigma'] = [\sigma] \\ 0 & \text{otherwise} \end{cases} \tag{A.11}$$

It can be shown that for any choice of inner product on $C^p(K, \mathbb{R})$, there exists a positive weight function $f : K \to \mathbb{R}_+ \setminus \{0\}$ satisfying:

$$\langle\, g, h \,\rangle_f = \sum_{\sigma \in K^p} f(\sigma) g([\sigma]) h([\sigma]) \tag{A.12}$$

Furthermore, the set of weight functions and scalar product on $C^p(K, \mathbb{R})$ wherein elementary cochains are orthogonal are in one-to-one correspondence []. Indeed, if $f : (\mathbb{R}^n, H_n) \to (\mathbb{R}^m, H_m)$ be a linear map between inner product matrices $H_n \in \mathbb{R}^{n \times n}$ and $H_m \in \mathbb{R}^{m \times m}$, then by Proposition [] for any $x \in \mathbb{R}^n$ and $y \in \mathbb{R}^m$, we have the following equivalence of inner products:

$$\langle fx, y \rangle_{\mathbb{R}^m} = \langle x, f^* y \rangle_{\mathbb{R}^n} = x^T F^T H_m y = x^T H_n F^* y$$

where $F \in \mathbb{R}^{m\times n}$ denotes the matrix representative of f and $F^* = H_n^{-1} F^T H_m$ a representative of the adjoint $f^* : (\mathbb{R}^m, H_m) \to (\mathbb{R}^n, H_n)$ of f. In this way, we say that the choice of weight function *induces* an inner product on $C^p(K, \mathbb{R})$[4]. In this way, we reduce the study of geometry to the study "weight functions" of laplacian operators.

Laplacian matvec

We first recall the characteristics of the graph Laplacians $x \mapsto Lx$ operation. Given a simple undirected graph $G = (V, E)$, let $A \in \{0,1\}^{n\times n}$ denote its binary adjacency matrix satisfying $A[i,j] = 1 \Leftrightarrow i \sim j$ if the vertices $v_i, v_j \in V$ are adjacent in G, and let $D = \mathrm{diag}(\{\deg(v_i)\})$ denote the diagonal *degree* matrix, where $\deg(v_i) = \sum_{j\neq i} A[i,j]$. The *graph Laplacian*'s adjacency, incidence, and element-wise definitions are:

$$L = D - A = \partial_1 \circ \partial_1^T\,, \qquad L\,[i,j] = \begin{cases} \deg(v_i) & \text{if } i = j \\ -1 & \text{if } i \sim j \\ 0 & \text{if } i \nsim j \end{cases} \tag{A.13}$$

Furthermore, by using the adjacency relation $i \sim j$ as in [12], the linear and quadratic forms of L may be succinctly expressed as:

$$(\,\forall\, x \in \mathbb{R}^n\,) \qquad (Lx)_i = \deg(v_i)\cdot x_i - \sum_{i\sim j} x_j\,, \qquad x^T L x = \sum_{i\sim j} (x_i - x_j)^2 \tag{A.14}$$

If G has m edges and n vertices taking labels in the set $[n]$, computing the product from (A.14) requires just $O(m)$ time and $O(n)$ storage via two edge traversals: one to accumulate vertex degrees and one to remove components from incident edges. By precomputing the degrees, the operation reduces further to a single $O(n)$ product and $O(m)$ edge pass, which is useful when repeated evaluation for varying x is necessary.

To extend the two-pass algorithm outlined above when $p > 0$, we first require a generalization of the path-connected relation from (A.14). Denote with $\mathrm{co}(\tau) = \{\,\sigma \in K^{p+1} \mid \tau \subset \sigma\,\}$ the set of proper cofaces of $\tau \in K^p$, or *cofacets*, and the (weighted) *degree* of $\tau \in K^p$ with:

$$\deg_w(\tau) = \sum_{\sigma\in \mathrm{co}(\tau)} w(\sigma)$$

Note setting $w(\sigma) = 1$ for all $\sigma \in K$ recovers the integral notion of degree representing the number of cofacets a given p-simplex has. Now, since K is a simplicial complex, if the faces τ, τ' share a common cofacet $\sigma \in K^{p+1}$, this cofacet $\{\sigma\} = \mathrm{co}(\tau) \cap \mathrm{co}(\tau')$ is in fact *unique* [19]. Thus, we may use a relation $\tau \overset{\sigma}{\sim} \tau'$ to rewrite the operator from (A.7) element-wise:

$$L_p^{\mathrm{up}}(\tau,\tau') = \begin{cases} \deg_w(\tau)\cdot w^+(\tau) & \text{if } \tau = \tau' \\ s_{\tau,\tau'}\cdot w^{+/2}(\tau)\cdot w(\sigma)\cdot w^{+/2}(\tau') & \text{if } \tau \overset{\sigma}{\sim} \tau' \\ 0 & \text{otherwise} \end{cases} \tag{A.15}$$

where $s_{\tau,\tau'} = \mathrm{sgn}([\tau], \partial[\sigma]) \cdot \mathrm{sgn}([\tau], \partial[\sigma])$. Ordering the p-faces $\tau \in K^p$ along a total order and choosing an indexing function $h : K^p \to [n]$ enables explicit computation of the corresponding matrix-vector product:

$$(L_p^{\mathrm{up}}\, x)_i = \deg_w(\tau)\cdot w(\tau)\cdot x_i + \sum_{\tau \overset{\sigma}{\sim} \tau'} s_{\tau,\tau'}\cdot x_{h(\tau')}\cdot w^{+/2}(\tau)\cdot w(\sigma)\cdot w^{+/2}(\tau') \tag{A.16}$$

Observe (A.16) can be evaluated now via a very similar two-pass algorithm as described for the graph Laplacian if the simplices of K^{p+1} can be quickly enumerated and the indexing function h can be efficiently evaluated.

[4] Nullspace comment

Lanczos

Computing eigen-decompositions $A = V\Lambda V^T$ of symmetric matrices $A \in S_n$ generally consists of two phases: (1) reduction to tridiagonal form $Q^T AQ = T$ via orthogonal similarity transformations Q, and (2) diagonalization of the tridiagonal form $T = Y\Theta Y^T$. While the latter may be performed in $O(n \log n)$ time [21], the former is effectively bounded below by $\Omega(n^3)$ for dense full-rank matrices using traditional (i.e. non-Strassen) matrix operations, and thus it is the reduction to tridiagonal form that dominates the computation. Lanczos [24] proposed the *method of minimized iterations*—now known as the *Lanczos method*—as an attractive alternative for reducing A into a tridiagonal form and thus revealing its spectrum.

The means by which the Lanczos method estimates eigenvalues is by projecting onto successive Krylov subspaces. Given a large, sparse, symmetric $n \times n$ matrix A with eigenvalues $\lambda_1 \geq \lambda_2 > \cdots \geq \lambda_r > 0$ and a vector $v \neq 0$, the order-j Krylov subspaces of the pair (A, v) are the spaces spanned by:

$$\mathcal{K}_j(A, v) := \text{span}\{v, Av, A^2v, \ldots, A^{j-1}v\} = \text{range}(K_j(A, v)) \tag{A.17}$$

where $K_j(A, v) = [v \mid Av \mid A^2v \mid \cdots \mid A^{j-1}v]$ are their corresponding Krylov matrices. Krylov subspaces arise naturally from using the minimal polynomial of A to express A^{-1} in terms of powers of A. In particular, if A is nonsingular and its minimal polynomial has degree m, then $A^{-1}v \in K_m(A, v)$ and $K_m(A, v)$ is an invariant subspace[5] of A. Since A is symmetric, the spectral theorem implies that A is orthogonally diagonalizable and that we may obtain $\Lambda(A)$ by generating an orthonormal basis for $\mathcal{K}_n(A, v)$. To do this, the Lanczos method constructs successive QR factorizations of $K_j(A, v) = Q_j R_j$ for each $j = 1, 2, \ldots, n$. Due to A's symmetry and the orthogonality of Q_j, the identity $q_k^T Aq_l = q_l^T A^T q_k = 0$ is satisfied for all $k > l + 1$, giving the corresponding $T_j = Q_j^T AQ_j$ a tridiagonal structure:

$$T_j = \begin{bmatrix} \alpha_1 & \beta_1 & & & \\ \beta_1 & \alpha_2 & \beta_2 & & \\ & \beta_2 & \alpha_3 & \ddots & \\ & & \ddots & \ddots & \beta_{j-1} \\ & & & \beta_{j-1} & \alpha_j \end{bmatrix}, \ \beta_j > 0, \ j = 1, 2, \ldots, n \tag{A.18}$$

Unlike the spectral decomposition $A = V\Lambda V^T$—which identifies a diagonalizable A with its spectrum $\Lambda(A)$ up to a change of basis $A \mapsto M^{-1}AM$—there is no canonical choice of T_j due to the arbitrary choice of v. However, there is a connection between the iterates $K_j(A, v)$ and the full tridiagonalization of A: if $Q^T AQ = T$ is tridiagonal and $Q = [\, q_1 \mid q_2 \mid \cdots \mid q_n \,]$ is an $n \times n$ orthogonal matrix $QQ^T = I_n = [e_1, e_2, \ldots, e_n]$, then:

$$K_n(A, q_1) = QQ^T K_n(A, q_1) = Q[\, e_1 \mid Te_1 \mid T^2e_1 \mid \cdots \mid T^{n-1}e_1 \,] \tag{A.19}$$

is the QR factorization of $K_n(A, q_1)$—that is, tridiagonalizing A with respect to a unit-norm q_1 determines Q. Indeed, the Implicit Q Theorem [20] asserts that if an upper Hessenburg matrix $T \in \mathbb{R}^{n \times n}$ has only positive elements on its first subdiagonal and there exists an orthogonal matrix Q such that $Q^T AQ = T$, then Q and T are *uniquely* determined by (A, q_1). As a result, given an initial pair (A, q_1) satisfying $\|q_1\| = 1$, we may restrict and project A to its j-th Krylov subspace T_j via:

$$AQ_j = Q_j T_j + \beta_j q_{j+1} e_j^T \qquad (\beta_j > 0) \tag{A.20}$$

where $Q_j = [\, q_1 \mid q_2 \mid \cdots \mid q_j \,]$ is an orthonormal set of vectors mutually orthogonal to q_{j+1}. Equating the j-th columns on each side of (A.20) and rearranging the terms yields the *three-term recurrence*:

$$\beta_j \, q_{j+1} = Aq_j - \alpha_j \, q_j - \beta_{j\text{-}1} \, q_{j\text{-}1} \tag{A.21}$$

where $\alpha_j = q_j^T Aq_j$, $\beta_j = \|r_j\|_2$, $r_j = (A - \alpha_j I)q_j - \beta_{j\text{-}1}q_j$, and $q_{j+1} = r_j/\beta_j$. Equation (A.21) is a variable-coefficient second-order linear difference equation, and it is a known fact that such equations have unique solutions: if $(q_{j\text{-}1}, \beta_j, q_j)$ are known, then $(\alpha_j, \beta_{j+1}, q_{j+1})$ are completely determined. The sequential process that iteratively builds T_j via the recurrence from (A.21) is called the *Lanczos iteration*. Note that if A is

[5] Recall that if $S \subseteq \mathbb{R}^n$, then S is called an *invariant subspace* of A or *A-invariant* iff $x \in A \implies Ax \in S$ for all $x \in S$.

singular and we encounter $\beta_j = 0$ for some $j < n$, then $\text{range}(Q_j) = \mathcal{K}_j(A, q_1)$ is an A-invariant subspace, the iteration stops, and we have solved the symmetric eigenvalue problem: $\Lambda(T_j) = \Lambda(A)$, $j = \text{rank}(A)$, and T_j is orthogonally similar to A.

The Lanczos iteration and its many variants are part of a family of so-called "matrix free" spectral methods—the only aspect of the computation that depends on A is the matrix-vector product operator $v \mapsto Av$. Indeed, as A is not modified during the computation, the iteration may be executed without explicitly storing A in memory. Moreover, the three-term recurrence from (A.21) implies each iteration requires just three $O(n)$-sized vectors and a few $O(n)$ vector operations, justifying the following proposition:

Proposition 10 ([28, 34])**.** *Given a symmetric rank-r matrix $A \in \mathbb{R}^{n\times n}$ whose matrix-vector operator $A \mapsto Ax$ requires $O(\eta)$ time and $O(\nu)$ space, the Lanczos iteration computes $\Lambda(A) = \{\lambda_1, \lambda_2, \ldots, \lambda_r\}$ in $O(\max\{\eta, n\} \cdot r)$ time and $O(\max\{\nu, n\})$ space, when computation is done in exact arithmetic.*

As in [28], the assumption of exact arithmetic simplifies both the presentation of the theory and the corresponding complexity statements. Although this assumption is unrealistic in practical settings, it gives us a grounded expectation of what is possible to achieve with any *finite-precision* algorithm based on the Lanczos method: any implementation that computes $\Lambda(A) = \{\lambda_1, \lambda_2, \ldots, \lambda_r\}$ using the Lanczos iteration in finite-precision arithmetic must require $\Omega(\max\{\eta, n\} \cdot r)$ time and $\Omega(\max\{\nu, n\})$ space complexity.

In practice, finite-precision arithmetic introduces both rounding and cancellation errors into the computation, which manifests as loss of orthogonality between the Lanczos vectors. These errors not only affect the methods convergence rate towards an invariant subspace, but in fact they muddle the termination condition entirely. As a result, several decades of research have been dedicated to developing orthogonality-enforcement schemes that retain the simplicity of the Lanczos iteration without increasing either the time or space complexities by non-trivial factors. As these extensions are complex, multifaceted, and beyond the scope of the present work, we defer their discussion to the appendix A.3 and refer the curious reader to [20, 28, 34] and references therein for an overview.

Directional Transform

The canonical interpretation of the information displayed by a persistence diagram is that is summarizes the persistence of the sublevel sets of filtered space. Given a filtration pair (K, f) where K is a finite simplicial complex and $f : K \to \mathbb{R}$ is a real-valued function, the sublevel sets $|K|_i = f^{-1}(-\infty, i]$ deformation retract to... If K is embedded in $\mathbb{R}^d$, then geometrically f takes on the interpretation of a 'height' function whose range yields the 'height' of every simplex in K.

Let $X \subset \mathbb{R}^d$ denote a data set which can be written as a finite simplicial complex K whose simplices are PL-embedded in $\mathbb{R}^d$. Given this setting, define the *directional transform* (DT) of K as follows:

$$\begin{aligned} \text{DT}(K) : S^{d-1} &\to K \times C(K, \mathbb{R}) \\ v &\mapsto (K_\bullet, f_v) \end{aligned}$$

where we write $(K_\bullet, f)$ to indicate the filtration on K induced by f_v for all $\alpha \in \mathbb{R}$, i.e.:

$$K_\bullet = K(v)_\alpha = \{\, x \in X \mid \langle x, v\rangle \leq \alpha \,\} \tag{A.22}$$

Conceptually, we think of DT as an S^{d-1}-parameterized family of filtrations.

The Persistent Homology Transform (PHT) is a shape statistic that establishes a fundamental connection between the topological information summarized by K's PH groups and the geometry of its associated embedding. Given a complex K built from X, it is defined as:

$$\begin{aligned} \text{PHT}(K) : S^{d-1} &\to \mathcal{D}^d \\ v &\mapsto \big(\, \text{dgm}_0(K, v), \text{dgm}_1(K, v), \ldots, \text{dgm}_{d-1}(K, v) \,\big) \end{aligned} \tag{A.23}$$

where $\mathcal{D}$ denotes the space of p-dimensional persistence diagrams, for all $p = 0, \ldots, d-1$ and S^{d-1} the unit $d-1$ sphere. The stability of persistence diagrams ensures that the map $v \mapsto \text{dgm}_p(K, v)$ is Lipschitz with respect to the bottleneck distance metric $d_B(\cdot, \cdot)$ whenever K is a finite simplicial complex. Thus, the PHT may be thought of as an element in $C(S^{d-1}, \mathcal{D}^d)$: .

The primary result of [] is that the PHT is injective on the space of subsets of R^d that can be written as finite simplicial complexes[6], which we denote as $\mathcal{K}_d$. Equivalently, $\mathcal{K}_d$ decomposes space of all pairs (K, f) under the equivalence $(K, f) \sim (K, f')$ when $f(K) = f'(K)$.

A.2 Complexity of Persistence & Related work

We briefly recount the main complexity results of the persistence computation. With a few key exceptions, the majority of persistent homology implementations and extensions is based on the *reduction algorithm* introduced by Edelsbrunner and Zomorodian [18]. This algorithm factorizes the filtered boundary into a decomposition $R = \partial V$, where V is full rank upper-triangular and R is said to be in reduced form: if its i-th and j-th columns are nonzero, then $\mathrm{low}_R(i) \neq \mathrm{low}_R(j)$, where $\mathrm{low}_R(i)$ denotes the row index of the lowest non-zero in column i. We refer to [18, 3, 15] for details.

Given a filtration (K, f) of size $m = |K|$ with filter $f : K \to [m]$, the reduction algorithm in form given in [18] computes $\mathrm{dgm}_p(K; \mathbb{Z}/2) = \{ (\tau_1, \sigma_1), (\tau_2, \sigma_2), \ldots, (\tau_k, \sigma_k) \}$ runs in time proportional to the sum of the squared (index) persistences $\sum_{i=1}^{k} (f(\sigma_i) - f(\tau_i))^2$. As k is at most $m/2$, this implies a $O(m^3)$ upper bound on the complexity of the general persistence computation, which incidentally Morozov showed was a tight $\Theta(m^3)$ under the assumption that each column reduction takes $O(m)$ time. By exploiting the matrix-multiplication results, a similar result can be shown to reduce to $O(m^\omega)$, where ω is the matrix-multiplication constant, which is ≈ 2.37 as of this time of writing. It worth remarking that the complexity statements above are all given in terms of the number of *simplices* m: if $n = |K^0|$ is the size of the vertex set, the above implies a worst-case bound of $O(n^{\omega(p+2)})$ on the general persistence computation. For example, if we use non-Strassen-based matrix multiplication ($\omega = 3$) and we are concerned with $p = 1$ homology computation, the complexity of the reduction algorithm scales $O(n^9)$ in the number of vertices of the complex, which is essentially intractable for most real world application settings.

Despite the seemingly immense intractability of the persistence computation, decades of advancements have been made in reducing the complexity or achieving approximate results in reasonable time and space complexities. The complexity of the reduction algorithm is complicated by the fact that it depends heavily on the structure of the associated filtration K, the homology dimension p, the field of coefficients $\mathbb{F}$, and the assumptions about the space K manifests from. In [], Sheehy presented an algorithm for producing a sparsified version $(\tilde{K}, \tilde{f})$ of a given Vietoris-Rips filtration (K, f) constructed from an n-point metric space (X, d_X) whose total number of p-simplices is bounded above by $n \cdot (\epsilon^{-1})^{O(pd)}$, where d is the doubling dimension of X. It was shown that $\mathrm{dgm}_p(\tilde{K})$ is guaranteed to be a multiplicative c-approximation to the $\mathrm{dgm}_p(K)$, where $c = (1 - 2\epsilon)^{-1}$ and $\epsilon \leq 1/3$ is a positive approximation parameter. When $p = 0$ and the filtration function $f : K \to \mathbb{R}$ is PL, the reduction algorithm can be bypassed entirely in favor of simple $O(n \log n + \alpha(n)m) \approx O(m)$ algorithm (see Algorithm 5 in [15]), where $n = |K^0|$ and $m = |K^1|$ and $\alpha(n)$ is the extremely slow-growing inverse Ackermann function. Moreover, the $d-1$ persistence pairs can be computed in $O(n\alpha(n))$ time algorithm for filtrations of simplicial d-manifolds essentially reducing the problem to computing persistence on a dual graph [15]. For clique complexes, the apparent pairs optimization—which preemptively removes zero-persistence pairs from the computation prior to the reduction—has been empirically observed to reduce the number of columns needing reduced for clique complexes by $\approx 98 - 99\%$ [3]. Numerous other optimizations, including e.g. the *clearing optimization*, the use of *cohomology*, the *implicit reduction* technique, have further reduced both the non-asymptotic constant factors of the reduction algorithm significantly, see [3] and references therein for a full overview.

Despite the dramatic reductions in time and space needed for the persistence algorithm to complete, to the author knowledge relatively little has been done in improving the complexity and effective runtime of the reduction in parameterized settings. Although both of these algorithms have shown significant constant-factor reductions in the (re)-reduction of the associated sparse matrices, all of the techniques require $O(m^2)$ storage to execute as the R and V matrices must be maintained throughout the computation. Moreover, all three of the above methods intrinsically work within the reduction framework, wherein simulating persistence in dynamic contexts effectively reduces to the combinatorial problem of maintaining a valid $R = \partial V$ decomposition.

[6] Implicit in the injectivity statement of the PHT is that, given a subset $X \subset \mathbb{R}^d$ which may be written as finite simplicial complex K, the restriction $f : X \to \mathbb{R}$ to any simplex in K must is linear.

As noted in [15], the reduction algorithm is essentially a variant of Gaussian elimination. Indeed, the persistence of a given filtration can be computed by the PLU factorization of a matrix. The explicit decompositional approach of factorizing a large matrix into constitutive parts is known historically in numerical linear algebra as a *direct method*—methods would yield the exact solution within a finite number of steps. In contrast, iterative methods start with approximate solution and progressively update the solution up to arbitrary accuracy. The iterative methods well-known to the numerical linear algebra community, such as Krylov methods, are typically often attractive not only due to the reduction in computational work over direct approaches but also of the limited amount of memory that is required. Despite the success of iterative methods in efficiently solving linear systems manifesting from diagonally dominant sparse matrices is [], such advancements have not yet been extended to the persistence setting.

Output sensitive multiplicity and Betti

We record this fact formally with two corollaries. Let $\mathrm{R}_p(k)$ denotes the complexity of computing the rank of square $k \times k$ matrix with at most $O((p+1)k)$ non-zero $\mathbb{F}$ entries. Then we have:

Corollary 2. *Given a filtration $K_\bullet$ of size $N = |K_\bullet|$ and indices $(i, j) \in \Delta_+^N$, computing $\beta_p^{i,j}$ using expression (2.11) requires $O\big(\max\{\mathrm{R}_p(n_i), \mathrm{R}_{p+1}(m_j)\}\big)$ time, where $n_i = |K_i^p|$ and $m_j = |K_j^{p+1}|$.*

Observe the relation $\partial_{p+1}^{i+1,j} \subseteq \partial_{p+1}^{1,j}$ implies the dominant cost of computing (2.11) lies in computing either $\mathrm{rank}(\partial_p^{1,i})$ or $\mathrm{rank}(\partial_{p+1}^{1,j})$, which depends on the relative sizes of $|K^p|$ and $|K^{p+1}|$. In contrast, μ_p^R is localized to the pair (K_i, K_l) and depends only on the $(p+1)$-simplices in the interval $[i, l]$, yielding the following corollary.

Corollary 3. *Given a filtration $K_\bullet$ of size $N = |K_\bullet|$ and a rectangle $R = [i, j] \times [k, l]$ with indices $0 \le i < j \le k < l \le N$, computing μ_p^R using expression (2.12) requires $O(\mathrm{R}_{p+1}(m_{il}))$ time $m_{il} = |K_l^{p+1}| - |K_i^{p+1}|$.*

A.3 Finite-precision arithmetic

It is well established in the literature that the Lanczos iteration, as given in its original form, it effectively useless in practice due to significant rounding and cancellation errors. Such errors manifest as loss of orthogonality between the computed Lanczos vectors, which drastically affects the convergence of the method. At first glance, this seems to be a simple numerical issue, however the analysis from Parlett [28] showed, loss of orthogonality is not merely the result of gradual accumulation of roundoff error—it is in fact is intricately connected to the convergence behavior of Lanczos iteration. One obvious remedy to this is to reorthogonalize the current Lanczos vectors $\{q_{j-1}, q_j, q_{j+1}\}$ against all previous vectors using Householder matrices [20]—a the *complete reorthogonalization* scheme. This process guarantees orthogonality to working precision, but incurs a cost of $O(jn)$ for each Lanczos step, effectively placing the iteration back into the cubic time and quadratic memory regimes the direct methods exhibit. A variety of orthogonality enforcement schemes have been introduced over years, including implicit restart schemes, selective reorthogonalization, thick restarts, block methods, and so on; see [] for an overview.

A.4 Laplacian Interpretation

In what follows we make a connection between boundary matrices and the graph Laplacian to illustrate how the Laplacian captures the "connectivity" aspects of the underlying simplicial complex.

Example A.1 (Adapted from [27])**.** Suppose the vertices of G are ordered and labeled from 1 to n arbitrarily such that, given any subset $X \subseteq V$, we may define column vector $x = (\, x_i \,)$ whose components $x_i = 1$ indicate $i \in X$ and $x_i = 0$ otherwise. Given such a set $X \subseteq V$, let $X' = V \setminus X$ denote its complement set. By L's definition, we have:

$$
\begin{aligned}
(Lx)_i > 0 &\iff i \in X \text{ and } |c_i(X)| = (Lx)_i \\
(Lx)_i < 0 &\iff i \in X' \text{ and } |c_i(X')| = |(Lx)_i| \\
(Lx)_i = 0 &\iff i \in X \cup X' \text{ and } c_i(X) = \emptyset
\end{aligned}
$$

where $c_v(X) = \{(v, w) \in E \mid v \in X \text{ and } w \in V \setminus X\}$ denotes the *cutset* of X restricted to v, i.e. the set of edges having as one endpoint $v \in X$ and another endpoint outside of X.

In other words, example A.1 demonstrates that L captures exactly how X is connected to the rest of G. Notice that if $X = V$, then $Lx = 0$ and thus 0 must be an eigenvalue of L with an eigenvector pair $\mathbf{1}$. Like the adjacency matrix, the interpretation of the matrix-vector product has a natural extension to powers of L, wherein just as entries in A^k model paths, entries in L^k are seen to model boundaries [27].

Parameterizing Settings

We include a few examples of potential application areas of work. Namely, we show a few promising examples of "parameterized settings" that may naturally benefit from our efforts here.

Dynamic Metric Spaces: Consider an $\mathbb{R}$-parameterized metric space $\delta_X = (X, d_X(\cdot))$ where X is a finite set and $d_X(\cdot) : \mathbb{R} \times X \times X \to \mathbb{R}_+$, satisfying:

1. For every $t \in \mathbb{R}, \delta_X(t) = (X, d_X(t))$ is a pseudo-metric space[7]
2. For fixed $x, x' \in X$, $d_X(\cdot)(x, x') : \mathbb{R} \to \mathbb{R}_+$ is continuous.

When the parameter $t \in \mathbb{R}$ is interpreted as *time*, the above yields a natural characterization of a "time-varying" metric space. More generally, we refer to an $\mathbb{R}^h$-parameterized metric space as *dynamic metric space*(DMS). Such space have been studied more in-depth [] and have been shown...

Rayleigh Ritz values Though the Lanczos iterations may be used to obtain the full tridiagonalization $A = QTQ^T$, intermediate spectral information is readily available in T_j, for $j < \text{rank}(A)$. Diagonalizing $T_j = Y\Theta Y^T$ yields value/vector pairs $\{(\theta_1^{(j)}, y_1^{(j)}), \ldots, (\theta_j^{(j)}, y_j^{(j)})\}$ satisfying $w^T(Ay - \theta y) = 0$ for all $w \in \mathcal{K}_j(A, q_1)$, called *Ritz pairs*. The values θ are called *Ritz values* and their associated vectors $v = Qy$ in the range of Q are called *Ritz vectors*. From the Ritz perspective, the Lanczos iteration implicitly maintains two orthonormal basis for $K_j(A, q_1)$—a Lanczos basis Q and the Ritz basis Y:

$$A = QTQ^T = QY\Theta Y^T Q^T \iff AQY = QY\Theta$$

In principle, the Lanczos basis $\{q_i\}_{i=1}^j$ changes each iteration, while the Ritz basis $\{Qy_i^{(j)}\}_{i=1}^j$ changes after each subspace projection. The way in which the Ritz values approach the spectrum of A is well-studied [], as they are known to be Rayleigh-Ritz approximations of A's eigenpairs $\Lambda(A) = \{(\lambda_1, v_1), \ldots, (\lambda_j, v_j)\}$, and they are collectively known to be optimal in the sense that $T_k = B$ is the matrix that minimizes $\|AQ_k - Q_k B\|_2$ over the space of all $k \times k$ matrices. Moreover, Ritz values contain intrinsic information of the distance between $\Lambda(T_j)$ and $\Lambda(A)$. To see this, note that:

$$\|Av_i^{(j)} - v_i^{(j)}\theta_i^{(j)}\| = \beta_i^{(j)} = \beta_{j+1} \cdot |\langle e_j, y_i^{(j)}\rangle| \tag{A.24}$$

Thus, we need not necessarily keep the Lanczos vectors Q in memory to monitor how close the spectra of the T_j's approximate $\Lambda(A)$. In fact, it is known that the Ritz values $\{\theta_1^{(1)}, \theta_1^{(2)}, \ldots, \theta_1^{(j)}\}$ of T_j satisfy:

$$|\lambda - \theta_i^{(j)}| \leq \left(\beta_i^{(j)}\right)^2 / \left(\min_{\mu} |\mu - \theta_i^{(j)}|\right) \tag{A.25}$$

The full convergence of the Ritz values to the eigenvalues of A is known to converge at a rate that depends on the ratio between λ_1/λ_n. A full analysis is done in terms of Chebychev Polyonomials in [20]. In practice, it has been observed that the Lanczos iteration converges super-linearly towards the extremal eigenvalues of the spectrum, whereas for interior eigenvalues one typically must apply a shifting scheme.

[7] This is required so that if one can distinguish the two distinct points $x, x' \in X$ incase $d_X(t)(x, x') = 0$ at some $t \in \mathbb{R}$.

Convergence Rate

The ability of the Krylov subspace iteration to capture the extremal portions of the spectrum remains unparalleled, and by using $O(n)$ memory, the Lanczos iteration uses optimal memory. As mentioned in section **??**, when the computation is carried out in finite-precision arithmetic, one may observe loss of orthogonality in the Lanczos vectors. Fortunately, the connection between the Lanczos method and the Rayleigh quotient ensures *eventual* termination of the procedure under by restarting the Lanczos method, and continue with the iteration until the spectrum has been approximated to some prescribed accuracy. Unfortunately, if the number of iterations k is e.g. larger than n^2, then the method may approach to $O(r \max(\mathcal{M}(n), n), n) \approx O(n^3)$ complexity one starts with. If the supplied matrix-vector product operation is fast, the number of iterations k needed for convergence of the Lanczos method becomes the main bottleneck estimating the spectrum of A.

Loss of orthogonality can be mitigated by re-orthogonalizaing against all previous Lanczos vectors, but this increases the Lanczos complexity to $\approx O(n^2)$ per iteration. Thus, the goal is strike a balance: find a way to keep all n Lanczos numerically orthonormal, so as to ensure super-linear convergence of the Ritz values θ, but do so using $c \cdot n$ memory, where c is a relatively small constant.

Since rates of convergence α increases the number of correct digits by an expoentnial rate with factor *alpha*, any super-linear convergent ($\alpha > 1$) method needs at most c terms to approximate an eigen-pair up to numerical precision. In the context of the Lanczos method, achieving even quadratic convergence would imply the number of iterations needed to obtain machine-precision is bounded by $T(c \cdot \mathcal{M}(n) \cdot r)$, where c is a small constant. We say that a method which achieves *superlinear* convergence has complexity *essentially* $O(c \cdot n) \approx O(n)$.

Among the more powerful methods for achieving super linear convergence towards a given eigenvalue λ is the Jacobi-Davidson method. This method seeks to correct:

Solving for t results in the *correction equation*

$$(I - uu^T)(A - \sigma I)(I - uu^T)t = \theta u - Au \tag{A.26}$$

where, since u is unit-norm, $I - uu^T$ is a projector onto the complement of span(u). It's been shown that solving exactly for this correction term essentially constructs an cubically-convergent sequence towards some $\theta \mapsto \lambda$ in the vicinity of σ. Solving for the correction equation exactly is too expensive, sparking efforts to approximate it. It turns out that, just as the Lanczos method in exact arithmetic is highly related to the conjugate gradient method for solving linear systems, solving for the correction equation exactly is in some ways conceptually similar to making an Newton step in the famous Newtons method from nonlinear optimization. Since (**??**) is approximated, the JD method is often called in the literature akin to making an "inexact newton step" [].

The JD method with inexact Newton steps yields an individual eigenvalue estimate with quadratic convergence—*essentially* $O(m)$ time after some constant number matrix-vector products and $O(n)$ memory. The Lanczos method, in contrast, estimates all eigenvalues in essentially quadratic time if the convergence rate is superlinear. Pairing these two methods is a non-trivial endeavor. In a sequence of papers, Stathopoulos et al [] investigated various strategies for approximately solving the correction equation. In , they give both theoretical and empricial evidence to suggest that by employing generalized Davidson and Jacobi-Davidson like solvers within an overarching Lanczos paradigm, they achieve nearly optimal methods for estimating large portions of the spectrum using $O(1)$ number of basis vectors. By approximating the inner iterations with the symmetric Quasi-Minimal Residual (QMR) method, they argue that JD cannot converge more than three times slower than the optimal method, and empirically they find the constant factor to be less than 2.

A common way of quantifying the sensitivity of the spectrum of a given linear operator M is through its condition number. For $M = XX^T$ a given positive definite matrix, its *condition number* $\kappa(M)$ is defined as:

$$\kappa(M) = \|M^{-1}\|\|M\| = |\lambda_1(M)| \,/\, |\lambda_n(M)| \tag{A.27}$$

The condition number $\kappa(M)$ directly measures of how sensitive the spectrum of M is too perturbations in its entries. In particular, if $E \in \mathbb{R}^{n \times n}$ represents a small perturbation of $M \in \mathbb{R}^{n \times n}$, then:

$$\frac{\|(M + E)^{-1} - M^{-1}\|}{\|M^{-1}\|} \leq \kappa(M) \frac{\|E\|}{\|M\|} \tag{A.28}$$

Thus, the effect of adding ϵI_n to a given matrix can be interpreted as a means of reducing κ arbitrarily—at the expense of accuracy—to stabilize the pseudo-inverse. For operators $\Phi_\epsilon(\cdot)$ in the form above, we can quantify this stabilization using perturbation analysis.

A.5 Proofs

Proof of rank equivalence

In general, it is not true that $\text{rank}(A) = \text{rank}(\text{sgn}(A))$. However, it is true that $\text{rank}(\partial_p) = \text{rank}(\text{sgn}(\partial_p))$.

Proof of Lemma 1

Proof. The Pairing Uniqueness Lemma [15] asserts that if $R = \partial V$ is a decomposition of the total $m \times m$ boundary matrix ∂, then for any $1 \leq i < j \leq m$ we have $\text{low}_R[j] = i$ if and only if $r_\partial(i,j) = 1$. As a result, for $1 \leq i < j \leq m$, we have:

$$\text{low}_R[j] = i \iff r_R(i,j) \neq 0 \iff r_\partial(i,j) \neq 0 \tag{A.29}$$

Extending this result to equation (2.10) can be seen by observing that in the decomposition, $R = \partial V$, the matrix V is full-rank and obtained from the identity matrix I via a sequence of rank-preserving (elementary) left-to-right column additions. □

Proof of Proposition 1

Proof. We first need to show that $\beta_p^{i,j}$ can be expressed as a sum of rank functions. Note that by the rank-nullity theorem, so we may rewrite (2.7) as:

$$\beta_p^{i,j} = \dim\left(C_p(K_i)\right) - \dim\left(B_{p-1}(K_i)\right) - \dim\left(Z_p(K_i) \cap B_p(K_j)\right)$$

The dimensions of groups $C_p(K_i)$ and $B_p(K_i)$ are given directly by the ranks of diagonal and boundary matrices, yielding:

$$\beta_p^{i,j} = \text{rank}(I_p^{1,i}) - \text{rank}(\partial_p^{1,i}) - \dim\left(Z_p(K_i) \cap B_p(K_j)\right)$$

To express the intersection term, note that we need to find a way to express the number of p-cycles born at or before index i that became boundaries before index j. Observe that the non-zero columns of R_{p+1} with index at most j span $B_p(K_j)$, i.e $\{\, \text{col}_{R_{p+1}[k]} \neq 0 \mid k \in [j] \,\} \in \text{Im}(\partial_{p+1}^{1,j})$. Now, since the low entries of the non-zero columns of R_{p+1} are unique, we have:

$$\dim(Z_p(K_i) \cap B_p(K_i)) = |\Gamma_p^{i,j}| \tag{A.30}$$

where $\Gamma_p^{i,j} = \{\, \text{col}_{R_{p+1}[k]} \neq 0 \mid k \in [j],\, 1 \leq \text{low}_{R_{p+1}}[k] \leq i \,\}$. Consider the complementary matrix $\bar{\Gamma}_p^{i,j}$, given by the non-zero columns of R_{p+1} with index at most j that are not in $\Gamma_p^{i,j}$, i.e. the columns satisfying $\text{low}_{R_{p+1}}[k] > i$. Combining rank-nullity with the observation above, we have:

$$|\bar{\Gamma}_p^{i,j}| = \dim(B_p(K_j)) - |\Gamma_p^{i,j}| = \text{rank}(R_{p+1}^{i+1,j}) \tag{A.31}$$

Combining equations (A.30) and (A.31) yields:

$$\dim(Z_p(K_i) \cap B_p(K_j)) = |\Gamma_p^{i,j}| = \dim(B_p(K_j)) - |\bar{\Gamma}_p^{i,j}| = \text{rank}(R_{p+1}^{1,j}) - \text{rank}(R_{p+1}^{i+1,j}) \tag{A.32}$$

Observing the final matrices in (A.32) are *lower-left* submatrices of R_{p+1}, the final expression (2.11) follows by applying Lemma 1 repeatedly. □

Proof of boundary matrix properties

Proof. First, consider property (1). For any $t \in T$, applying the boundary operator ∂_p to $K_t = \text{Rips}_\epsilon(\delta_{\mathcal{X}}(t))$ with non-zero entries satisfying (**??**) by definition yields a matrix ∂_p satisfying $\text{rank}(\partial_p) = \dim(\text{B}_{p-1}(K_t))$. In contrast, operators of the from (3.3) always produce p-boundary matrices of Δ_n; however, notice that the only entries which are non-zero are precisely those whose simplices σ that satisfy $\text{diam}(\sigma) < \epsilon$. Thus, $\text{rank}(\partial_p^t) = \dim(\text{B}_{p-1}(K_t))$ for all $t \in T$. < (show proof of (2))> Property (3) follows from the construction of ∂_p and from the inequality $\|A\|_2 \leq \sqrt{m}\|A\|_1$ for an $n \times m$ matrix A, as $\|\partial_p^t\|_1 \leq (p+1)\,\epsilon$ for all $t \in T$.

□

References

[1] Henry Adams, Tegan Emerson, Michael Kirby, Rachel Neville, Chris Peterson, Patrick Shipman, Sofya Chepushtanova, Eric Hanson, Francis Motta, and Lori Ziegelmeier. Persistence images: A stable vector representation of persistent homology. *Journal of Machine Learning Research*, 18, 2017.

[2] Ulrich Bauer. Ripser: efficient computation of vietoris–rips persistence barcodes. *Journal of Applied and Computational Topology*, 5(3):391–423, 2021.

[3] Ulrich Bauer and Michael Lesnick. Persistence diagrams as diagrams: A categorification of the stability theorem. In *Topological Data Analysis*, pages 67–96. Springer, 2020.

[4] Ulrich Bauer, Talha Bin Masood, Barbara Giunti, Guillaume Houry, Michael Kerber, and Abhishek Rathod. Keeping it sparse: Computing persistent homology revised. *arXiv preprint arXiv:2211.09075*, 2022.

[5] Rajendra Bhatia. *Matrix analysis*, volume 169. Springer Science & Business Media, 2013.

[6] Shujun Bi, Le Han, and Shaohua Pan. Approximation of rank function and its application to the nearest low-rank correlation matrix. *Journal of Global Optimization*, 57(4):1113–1137, 2013.

[7] Peter Bubenik et al. Statistical topological data analysis using persistence landscapes. *J. Mach. Learn. Res.*, 16(1):77–102, 2015.

[8] Andrea Cerri, Barbara Di Fabio, Massimo Ferri, Patrizio Frosini, and Claudia Landi. Betti numbers in multidimensional persistent homology are stable functions. *Mathematical Methods in the Applied Sciences*, 36(12):1543–1557, 2013.

[9] Frédéric Chazal, David Cohen-Steiner, Leonidas J Guibas, Facundo Mémoli, and Steve Y Oudot. Gromov-hausdorff stable signatures for shapes using persistence. In *Computer Graphics Forum*, volume 28, pages 1393–1403. Wiley Online Library, 2009.

[10] Frédéric Chazal, Vin De Silva, Marc Glisse, and Steve Oudot. *The structure and stability of persistence modules*, volume 10. Springer, 2016.

[11] Chao Chen and Michael Kerber. An output-sensitive algorithm for persistent homology. In *Proceedings of the twenty-seventh annual symposium on Computational geometry*, pages 207–216, 2011.

[12] Fan RK Chung. *Spectral graph theory*, volume 92. American Mathematical Soc., 1997.

[13] David Cohen-Steiner, Herbert Edelsbrunner, and John Harer. Stability of persistence diagrams. In *Proceedings of the twenty-first annual symposium on Computational geometry*, pages 263–271, 2005.

[14] David Cohen-Steiner, Herbert Edelsbrunner, and Dmitriy Morozov. Vines and vineyards by updating persistence in linear time. In *Proceedings of the twenty-second annual symposium on Computational geometry*, pages 119–126, 2006.

[15] Tamal Krishna Dey and Yusu Wang. *Computational topology for data analysis*. Cambridge University Press, 2022.

[16] Chao Ding, Defeng Sun, Jie Sun, and Kim-Chuan Toh. Spectral operators of matrices. *Mathematical Programming*, 168(1):509–531, 2018.

[17] Herbert Edelsbrunner and John L Harer. *Computational topology: an introduction*. American Mathematical Society, 2022.

[18] Herbert Edelsbrunner, David Letscher, and Afra Zomorodian. Topological persistence and simplification. In *Proceedings 41st annual symposium on foundations of computer science*, pages 454–463. IEEE, 2000.

[19] Timothy E Goldberg. Combinatorial laplacians of simplicial complexes. *Senior Thesis, Bard College*, 6, 2002.

[20] Gene H Golub and Charles F Van Loan. *Matrix computations*. JHU press, 2013.

[21] Ming Gu and Stanley C Eisenstat. A divide-and-conquer algorithm for the symmetric tridiagonal eigenproblem. *SIAM Journal on Matrix Analysis and Applications*, 16(1):172–191, 1995.

[22] Danijela Horak and Jürgen Jost. Spectra of combinatorial laplace operators on simplicial complexes. *Advances in Mathematics*, 244:303–336, 2013.

[23] Woojin Kim and Facundo Mémoli. Spatiotemporal persistent homology for dynamic metric spaces. *Discrete & Computational Geometry*, 66:831–875, 2021.

[24] Cornelius Lanczos. An iteration method for the solution of the eigenvalue problem of linear differential and integral operators. 1950.

[25] Olvi Mangasarian and Chunhui Chen. A class of smoothing functions for nonlinear and mixed complementarity problems. Technical report, 1994.

[26] Facundo Mémoli, Zhengchao Wan, and Yusu Wang. Persistent laplacians: Properties, algorithms and implications. *SIAM Journal on Mathematics of Data Science*, 4(2):858–884, 2022.

[27] Michael William Newman. The laplacian spectrum of graphs. Master's thesis, 2001.

[28] Beresford N Parlett. Do we fully understand the symmetric lanczos algorithm yet. *Brown et al*, 3:93–107, 1994.

[29] Jose A Perea. Persistent homology of toroidal sliding window embeddings. In *2016 IEEE International Conference on Acoustics, Speech and Signal Processing (ICASSP)*, pages 6435–6439. IEEE, 2016.

[30] Jose A Perea, Elizabeth Munch, and Firas A Khasawneh. Approximating continuous functions on persistence diagrams using template functions. *Foundations of Computational Mathematics*, pages 1–58, 2022.

[31] Matthew Piekenbrock and Jose A Perea. Move schedules: Fast persistence computations in coarse dynamic settings. *arXiv preprint arXiv:2104.12285*, 2021.

[32] Chi Seng Pun, Kelin Xia, and Si Xian Lee. Persistent-homology-based machine learning and its applications–a survey. *arXiv preprint arXiv:1811.00252*, 2018.

[33] Luis Scoccola and Jose A Perea. Fibered: Fiberwise dimensionality reduction of topologically complex data with vector bundles. In *39th International Symposium on Computational Geometry (SoCG 2023)*. Schloss Dagstuhl-Leibniz-Zentrum für Informatik, 2023.

[34] Horst D Simon. Analysis of the symmetric lanczos algorithm with reorthogonalization methods. *Linear algebra and its applications*, 61:101–131, 1984.

[35] Afra Zomorodian and Gunnar Carlsson. Computing persistent homology. In *Proceedings of the twentieth annual symposium on Computational geometry*, pages 347–356, 2004.

A Boundary matrix factorization

Definition 2 (Boundary matrix decomposition)**.** Given a filtration $K_\bullet$ with m simplices, let ∂ denote its $m \times m$ filtered boundary matrix. We call the factorization $R = \partial V$ the *boundary matrix decomposition* of ∂ if:

I1. V is full-rank upper-triangular

I2. R satisfies $\text{low}_R[i] \neq \text{low}_R[j]$ iff its i-th and j-th columns are nonzero

where $\text{low}_R(i)$ denotes the row index of lowest non-zero entry of column i in R or null if it doesn't exist. Any matrix R satisfying property (I2) is said to be *reduced*; that is, no two columns share the same low-row indices.

B Laplacian facts

In general, the spectrum of the graph Laplacian L is unbounded, [] and instead many prefer to work within the "normalized" setting where eigenvalues are bounded. The *normalized Laplacian* $\mathcal{L}$ of a graph G is typically given as:

$$\mathcal{L}(G) = D^{-1/2} L D^{-1/2} \tag{B.1}$$

with the convention that $D^{-1}(v_i, v_i) = 0$ for $\deg(v_i) = 0$. The variational characterization of eigenvalues in terms of the Rayleigh quotient of $\mathcal{L}$ convey a particular form. Specifically, for any real-valued function $f : V \to \mathbb{R}$ on G, when viewed as a column vector, $\mathcal{L}$ satisfies:

$$\frac{\langle f, \mathcal{L} f \rangle}{\langle f, f \rangle} = \frac{\sum\limits_{i \sim j} (g(v_i) - g(v_j))^2}{\sum\limits_{i} g(v_i)^2 \cdot \deg(v_i)} \tag{B.2}$$

where $f = D^{1/2} g$ and $\langle f, g \rangle$ denotes the standard inner product in $\mathbb{R}^n$. Equation (B.2) may be used to show that the spectrum $\Lambda(\mathcal{L})$ is bounded in the interval $[0, 2]$. In particular, it is known that:

$$\lambda_i \leq \sup_f \frac{\langle f, \mathcal{L} f \rangle}{\langle f, f \rangle} \leq 2 \tag{B.3}$$

Recall that, when G is connected, 0 is an eigenvalue of both L and $\mathcal{L}(G)$, with multiplicity $\mathrm{cc}(G)$. Moreover, if G is the union of disjoint graphs $G_1, G_2, \ldots, G_k$, then it has as its spectrum the union of the spectra $\Lambda(G_1), \Lambda(G_2), \ldots, \Lambda(G_k)$. Certain parts of the spectrum of $\mathcal{L}$ can be deduced explicitly for very structured types of G, such as complete graphs, complete bipartite graphs, star graphs, path graphs, and cycle graphs, and n-cubes. For a list of additional properties the graph and normalized Laplacians satisfy, including bounds on eigenvalues, relation to random walks and rapidly-mixing Markov chains, identities tied to isoperimetric properties of graphs, and explicit connections to spectral Riemannian geometry, see [12] and references within.

C Laplacian `matvec` products

Below is pseudocode outlining how to evaluate a weighted (up) Laplacian matrix-vector multiplication built from a simplicial complex K with $m = |K^{p+1}|$ and $n = |K^p|$ in essentially $O(m)$ time when $m > n$ and p is considered a small constant. Key to the runtime of the operation being essentially linear is the constant-time determination of orientation between p-faces ($s_{\tau,\tau'}$)—which can be inlined during the computation—and the use of a deterministic $O(1)$ hash table $h : K^p \to [n]$ for efficiently determining the appropriate input/output offsets to modify (i and j). Note the degree computation occurs only once.

Algorithm 1 `matvec` for weighted p up-Laplacians in $O(m(p+1)) \approx O(m)$ time ($p \geq 0$)

Require: Fixed oriented complex K of size $N = |K|$
Optional: Weight functions $w_{p+1} : K^{p+1} \to \mathbb{R}_+$ and $w_p^l, w_p^r : K^p \to \mathbb{R}_+$
Output: $y = \langle L_p^{\text{up}}, x \rangle = (W_p \circ \partial_{p+1} \circ W_{p+1} \circ \partial_{p+1}^T \circ W_p)x$

```
1:  # Precompute weighted degrees deg_w
2:  h : K^p → [n]
3:  deg_w ← 0
4:  for σ ∈ K^{p+1} do:
5:      for τ ∈ ∂[σ] do:
6:          deg_w[h(τ)] ← deg_w[h(τ)] + w_p^l(τ) · w_{p+1}(σ) · w_p^r(τ)
7:
8:  function UpLaplacianMatvec(x ∈ R^n)
9:      y ← deg_w ⊙ x   (element-wise product)
10:     for σ ∈ K^{p+1} do:
11:         for τ, τ' ∈ ∂[σ] × ∂[σ] where τ ≠ τ' do:
12:             s_{τ,τ'} ← sgn([τ], ∂[σ]) · sgn([τ'], ∂[σ])
13:             i, j ← h(τ), h(τ')
14:             y_i ← y_i + s_{τ,τ'} · x_j · w_p^l(τ) · w_{p+1}(σ) · w_p^r(τ')
15:     return y
```

In general, the signs of the coefficients $\text{sgn}([\tau], \partial[\sigma])$ and $\text{sgn}([\tau'], \partial[\sigma])$ depend on the position of τ, τ' as summands in $\partial[\sigma]$ (2.2), which itself depends on the orientation of $[\sigma]$ (**??**). Thus, evaluation of these sign terms takes $O(p)$ time to determine for a given $\tau \in \partial[\sigma]$ with $\dim(\sigma) = p$, which if done naively via line (12) in the pseudocode C increases the complexity of the algorithm. However, observe that the sign of their product is in fact invariant in the orientation of $[\sigma]$ (see Remark 3.2.1 of [19])—thus, if we fix the orientation of the simplices of K^p, the sign pattern $s_{\tau,\tau'}$ for every $\tau \overset{\sigma}{\sim} \tau'$ can be precomputed and stored ahead of time, reducing the evaluation $s_{\tau,\tau'}$ to $O(1)$ time and $O(m)$ storage. Alternatively, if the labels of the $p+1$ simplices $\sigma \in K^{p+1}$ are given an orientation induced from the total order on V, then we can remove the storage requirement entirely and simply fix the sign pattern during the computation.

A subtle but important aspect of algorithmically evaluating (A.16) is the choice of indexing function $h : K^p \to [n]$. This map is necessary to deduce the contributions of the components x_* during the operation (line (13)). While this task may seem trivial as one may use any standard associative array to generate this map, typical implementations that rely on collision-resolution schemes such as open addressing or chaining only have $O(1)$ lookup time in expectation. Moreover, empirical testing suggests that line (13) in C can easily bottleneck the entire computation due to the scattered memory access such collision-resolution schemes may involve. One solution avoiding these collision resolution schemes that exploits the fact that K is fixed is to build an order-preserving *perfect minimal hash function* (PMHF) $h : K^p \to [n]$. It is known how to build PMHF's over fixed input sets of size n in $O(n)$ time and $O(n \log m)$ bits [], and such maps have deterministic $O(1)$ access time. Note that this process happens only once for a fixed simplicial complex K: once h has been constructed, it is fixed for every `matvec` operation.

D Parameterized setting & Perturbation theory

If f is a real-valued filter function that various smoothly in $\mathcal{H}$, one would expect the spectra of the constitutive terms in β_p^* and μ_p^* to also vary smoothly as functions of $\mathcal{H}$. Indeed, since Laplacian matrices are normal matrices, we expect their spectra to be quite stable under perturbations [].

Small condition numbers often improve the convergence of iterative solvers and improve stability of spectrum with respect to perturbations in the entries of the matrix. $\kappa(M^{-1}A)$

$$M^{-1}Ax = M^{-1}b$$

where M is symmetric positive definite.

$$\min_{x \perp \mathbf{1}} \frac{1}{2} x^T (L + \epsilon I_n) x - b^T x \tag{D.1}$$

Since this nonsingular, positive definite, strictly diagonally dominant matrix, thus we may apply the famous Conjugate Gradient (CG) algorithm to solve such a system. It's well known that CG converges to the solution of $Ax = b$ in exactly $O(n)$ iterations (and often much earlier), of which each iteration requires one $O(m)$ matrix-vector product, implying a runtime of $O(mn^2)$ (compare with...). Moreover, and since this is a Laplacian matrix, the wealth of tools developed for said matrices may also be used. In particular, [] showed that *low-stretch spanning trees* act as good preconditioners to accelerate Laplacian solvers, wherein it's been shown that the preconditioned Conjugate Gradient (PCG) requires as most $O(\sqrt{m} \log n)$ iterations, each of which requires one matrix-vector product using L_G and in $O(m^{1/3} \log n \ln 1/\epsilon)$ iterations. This was later improved by, who showed that one can solve Laplacian systems effectively in $O(m \log^{O(1)} n)$ time, giving a bound of $O(rm \log^{O(1)} n)$ time to obtain....

Of course, if one wants to compute either of the counting invariants in... exactly for $p = 0$, of course, the fastest algorithm is to reduce the problem to the well-known elder-rule problem, which takes $O(m \log m + m\alpha(n))$ time for a general filtration. It is unlikely that we may beat this bound, either in theory or in practice, for $p = 0$. However, the fastest known algorithm for computing the full persistence diagram for $p \geq 1$ is $O()$, which is quite a jump in complexity; there is no generalization of disjoint-set algorithm for the case where $p \geq 1$. Moreover, these direct methods tend to be memory bound operations, pushing researchers who want to compute these diagrams in practice to focus on ways of reducing the memory usage, such as using $\mathbb{Z}_2$ field coefficients. In contrast, the means by which we compute these invariants scales quite well with larger p, it produces a stronger invariant, and is far more reaching to other areas of mathematics.